

Synthesis and Comparative η^1 -Alkyl and Sterically Induced Reduction Reactivity of $(C_5Me_5)_3Ln$ Complexes of La, Ce, Pr, Nd, and Sm

William J. Evans,* Jeremy M. Perotti, Stosh A. Kozimor, Timothy M. Champagne, Benjamin L. Davis, Gregory W. Nyce, Cy H. Fujimoto, Robert D. Clark, Matthew A. Johnston, and Joseph W. Ziller

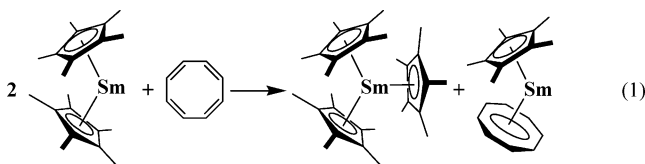
Department of Chemistry, University of California, Irvine, California 92697-2025

Received May 19, 2005

The synthesis of $(C_5Me_5)_3Ce$ and $(C_5Me_5)_3Pr$ from $[(C_5Me_5)_2Ln][(\mu-Ph)_2BPh_2]$ and KC_5Me_5 completes the series of sterically crowded $(C_5Me_5)_3Ln$ complexes for the larger lanthanides, La–Nd and Sm, and allows a comparison of structure and reactivity as a function of metal size. Synthesis of these new $(C_5Me_5)_3Ln$ complexes required silylated glassware, which surprisingly was not necessary for the more sterically crowded analogues. $(C_5Me_5)_3Ce$ and $(C_5Me_5)_3Pr$ display longer Ln–C(C_5Me_5) distances than any previously described Ce or Pr complexes containing the $(C_5Me_5)^-$ ligand. The η^1 - C_5Me_5 alkyl-like reactivity of the $(C_5Me_5)_3Ln$ complexes was investigated with CO, ethylene, THF, and H_2 . The sterically induced reduction (SIR) reactivity of the $(C_5Me_5)_3Ln$ complexes was examined with $Se=PPh_3$, $AgBPh_4$, C_8H_8 , and phenazine. All of these data indicate that $(C_5Me_5)_3Ln$ reactivity increases with decreasing size of the metal and hence increased steric crowding. The reactivity of $(C_5Me_5)_3Ln$ with CO_2 and with Et_3NHBPh_4 was examined since each substrate could react by either η^1 - C_5Me_5 alkyl or SIR pathways. In both cases, alkyl-like reactivity is observed: CO_2 forms the insertion product $(C_5Me_5)_2Ln(O_2CC_5Me_5)$, containing a carboxylate with a pentamethylcyclopentadiene substituent, and Et_3NHBPh_4 forms $[(C_5Me_5)_2Ln][(\mu-Ph)_2BPh_2]$ and C_5Me_5H . The reactions of $(C_5Me_5)_3Sm$ with aryl halides and primary alkyl halide radical clocks (RX) yield C_5Me_5R , C_5Me_5X , $(C_5Me_5)_2$, R–R, and $[(C_5Me_5)_xSmX_y]_z$ as products, which indicate that SIR is not the only reaction pathway with these substrates. The X-ray crystal structures of the $(C_5Me_5)_3Ln$ reaction products $[(C_5Me_5)_2La]_2(\mu-\eta^2:\eta^2-Se_2)$, $[(C_5Me_5)_2(THF)La]_2(\mu-\eta^2:\eta^2-Se_2)$, $[(C_5Me_5)_2La]_2(\mu-\eta^3:\eta^3-C_{12}N_2H_8)$, $[(C_5Me_5)_2Sm(\mu-I)]_3$, and $(C_5Me_5)_2Sm(O_2CC_5Me_5)$ are described as well as a new synthesis of $(C_5Me_5)_3Sm$ from $(C_5Me_5)_2Sm$ and $(C_5Me_5)_2$.

Introduction

The discovery of the first tris(pentamethylcyclopentadienyl) complex, $(C_5Me_5)_3Sm$,¹ eq 1, revealed new



opportunities in organometallic and cyclopentadienyl chemistry.² The synthesis and crystallographic characterization of this complex demonstrated that organometallic pentamethylcyclopentadienyl compounds could be isolated in which all the M–C bond distances are longer than conventional bond lengths. This is unusual particularly for the lanthanides, which typically have very regular and predictable metal–ligand bond distances.^{3–5} The reaction chemistry of $(C_5Me_5)_3Sm$ dem-

onstrated that such long-bond organometallic complexes have unusual reactivity.^{2,6–16}

Previously, $(C_5Me_5)_3M$ complexes were not expected to exist since the cone angle of a $(C_5Me_5)^-$ ligand was typically thought to be as large as 142° .¹⁷ This is much

(1) Evans, W. J.; Gonzales, S. L.; Ziller, J. W. *J. Am. Chem. Soc.* **1991**, *113*, 7423.

(2) Evans, W. J.; Davis, B. L. *Chem. Rev.* **2002**, *102*, 2119.

(3) Raymond, K. R.; Eigenbrot, C. W., Jr. *Acc. Chem. Res.* **1980**, *13*, 276.

(4) Evans, W. J.; Foster, S. E. *J. Organomet. Chem.* **1992**, *433*, 79.

(5) Williams, R. A.; Hanusa, T. P.; Huffman, J. C. *Organometallics* **1990**, *9*, 1128.

(6) Evans, W. J.; Forrestal, K. J.; Ziller, J. W. *J. Am. Chem. Soc.* **1995**, *117*, 12635.

(7) Evans, W. J.; Forrestal, K. J.; Ziller, J. W. *Angew. Chem., Int. Ed. Engl.* **1997**, *36*, 774.

(8) Evans, W. J.; Forrestal, K. J.; Ziller, J. W. *J. Am. Chem. Soc.* **1998**, *120*, 9273.

(9) Evans, W. J.; Forrestal, K. J.; Ansari, M. A.; Ziller, J. W. *J. Am. Chem. Soc.* **1998**, *120*, 2180.

(10) Evans, W. J.; Nyce, G. W.; Clark, R. D.; Doedens, R. J.; Ziller, J. W. *Angew. Chem., Int. Ed.* **1999**, *38*, 1801.

(11) Evans, W. J.; Nyce, G. W.; Ziller, J. W. *Angew. Chem., Int. Ed.* **2000**, *39*, 240.

(12) Evans, W. J.; Nyce, G. W.; Ziller, J. W. *J. Am. Chem. Soc.* **2000**, *122*, 12019.

(13) Evans, W. J.; Kozimor, S. A.; Nyce, G. W.; Ziller, J. W. *J. Am. Chem. Soc.* **2003**, *125*, 13831.

(14) Evans, W. J.; Kozimor, S. A.; Ziller, J. W. *J. Am. Chem. Soc.* **2003**, *125*, 14264.

(15) Evans, W. J.; Kozimor, S. A.; Ziller, J. W. *Polyhedron*, **2004**, *23*, 2689.

(16) Evans, W. J.; Kozimor, S. A.; Ziller, J. W. Kaltsoyannis, N. *J. Am. Chem. Soc.* **2004**, *126*, 14533.

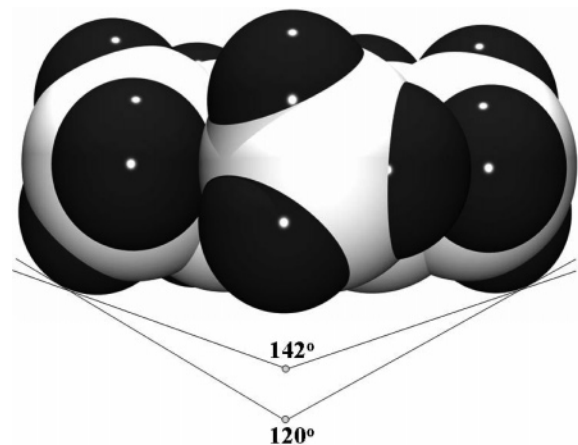
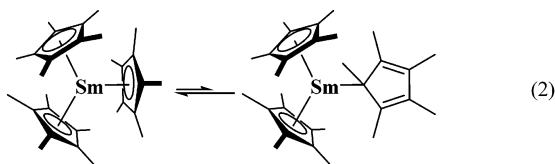


Figure 1. Comparison of (C₅Me₅)⁻ cone angles estimated at 142° and 120°.

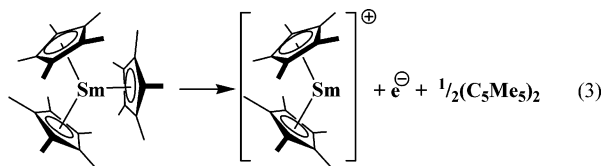
larger than the 120° angle needed for a (C₅Me₅)₃M complex. In (C₅Me₅)₃Sm, the (C₅Me₅)⁻ ligands can adopt a 120° cone angle because they are further away from the metal center than in normal trivalent samarium pentamethylcyclopentadienyl complexes, Figure 1. Hence, the Sm–C bond distances in (C₅Me₅)₃Sm are longer than those in trivalent (C₅Me₅)₂SmX (X = anion) complexes.⁴

Although (C₅Me₅)₃Sm is stable enough to be isolated and crystallographically characterized, it proved to be highly reactive.^{6–8} The observed reactivity necessarily involves the (C₅Me₅)⁻ rings since they are the only ligands. This reactivity is unusual since (C₅Me₅)⁻ is generally an inert ancillary ligand.^{18–20}

Two general modes of (C₅Me₅)₃Sm reactivity have been observed. With some substrates, (C₅Me₅)₃Sm reacted as if one of the (C₅Me₅)⁻ rings was an η¹-alkyl ligand, eq 2. Hence, the complex participates in olefin

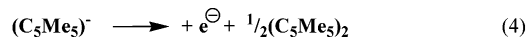


polymerization,⁷ CO insertion chemistry,⁶ and hydrogenolysis.⁸ In other cases, (C₅Me₅)₃Sm reacted as a one-electron reductant,⁸ eq 3. Since this reductive reactivity



is not observed in trivalent samarium pentamethylcyclopentadienyl complexes with normal Sm–C(C₅Me₅) bond distances, not even in the closely related ansa

complex, [Me₂Si(C₅Me₄)₂]Sm(C₅Me₅),²¹ the reactivity is likely to be due to steric crowding. Accordingly, this has been called sterically induced reduction (SIR).^{2,22} (C₅Me₅)₂²³ is considered the signature byproduct of this type of reduction which involves the half-reaction shown in eq 4. These reactions demonstrate that the reactivity



of the normally inert ancillary ligand, (C₅Me₅)⁻, can be substantially modified by creating a coordination environment in which the ligands have unusually long bonds.

Consistent with this view, preliminary studies of the reactivity of (C₅Me₅)₃Sm vs (C₅Me₅)₃Nd,¹⁰ a complex that contains a larger metal and is consequently less crowded, indicated that the amount of steric crowding would affect reactivity. One of the special advantages in lanthanide reaction chemistry is that the size of the metal can be varied to optimize a reaction within a given ligand set.^{2,22,24–26} Since there are 15 chemically similar trivalent lanthanide ions that gradually change in size with a range of only 0.17 Å (e.g., 1.14 Å (La) to 0.977 Å (Lu) for eight-coordinate trivalent radii),²⁷ metal size optimization can be quite precise with lanthanides. Moreover, in some cases the difference between the success or failure of a reaction depends on the size of the metal.^{28,29} If the reactivity of the (C₅Me₅)₃Ln complexes does depend heavily on steric crowding, reactivity should be controllable by varying the metal size.

This size optimization has special importance for the reductive chemistry observed for the (C₅Me₅)₃Ln complexes. Although metal-based size optimization can be accomplished for the trivalent Ln(III) ions, size optimization is not available for the reductive chemistry of the divalent lanthanide ions, since fewer examples of molecular Ln(II) ions are known and their chemistry differs.^{2,30,31} However, since sterically induced reduction brings divalent-like reductive chemistry to trivalent (C₅Me₅)₃Sm⁸ and (C₅Me₅)₃Nd,¹⁰ it was possible that size optimization of lanthanide reductive chemistry would be possible for all the lanthanides via this (C₅Me₅)₃Ln class of complexes.

To examine size optimization with (C₅Me₅)₃Ln complexes, examples of this class with the other lanthanide metals were required. Once (C₅Me₅)₃Sm was isolated,¹ it seemed sterically possible for other (C₅Me₅)₃Ln complexes to exist if the Ln was a metal larger than Sm, i.e., La, Ce, Pr, and Nd. The challenge was to find reaction pathways to the other (C₅Me₅)₃Ln complexes.

The reaction that generated (C₅Me₅)₃Sm, namely, the reduction of C₈H₈ by (C₅Me₅)₂Sm, eq 1, was successful since it formed a stable product, (C₅Me₅)₃Sm(C₈H₈), and

(17) Davies, C. E.; Gardiner, I. M.; Green, J. C.; Green M. L. H.; Hazel, N. J. Grebenik, P. D.; Mtetwa, V. S. B.; Prout, K. *J. Chem. Soc., Dalton Trans.* **1985**, 669.

(18) Crabtree, R. H. *The Organometallic Chemistry of the Transition Metals*, 3rd ed.; Wiley: New York, 2001; p 129.

(19) Bercaw, J. E. *J. Am. Chem. Soc.* **1974**, *96*, 5087.

(20) Schumann, H.; Meese-Marktscheffel, J. A.; Esser, L. *Chem. Rev.* **1995**, *95*, 865.

(21) Evans, W. J.; Cano, D. A.; Greci, M. A.; Ziller, J. W. *Organometallics* **1999**, *18*, 1381.

(22) Evans, W. J. *Coord. Chem. Rev.* **2000**, *206–207*, 263.

(23) Jutzi, P.; Kohl, F. *J. Organomet. Chem.* **1979**, *164*, 141.

(24) Evans, W. J. *Polyhedron* **1987**, *6*, 803.

(25) Evans, W. J. *Adv. Organomet. Chem.* **1985**, *24*, 131.

(26) Anwander, R.; Herrmann, W. A. *Top. Curr. Chem.* **1996**, *179*, 1.

(27) Shannon, R. D. *Acta Crystallogr.* **1976**, *A32*, 751.

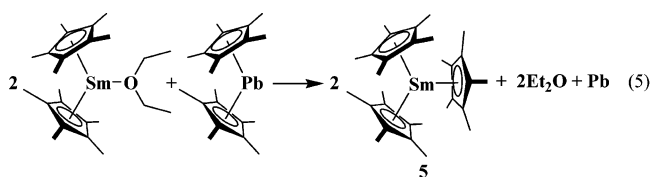
(28) Evans, W. J.; Dominguez, R.; Hanusa, T. P. *Organometallics* **1986**, *5*, 263.

(29) Alvarez, D.; Caulton, K. G.; Evans, W. J.; Ziller, J. W. *J. Am. Chem. Soc.* **1990**, *112*, 5674.

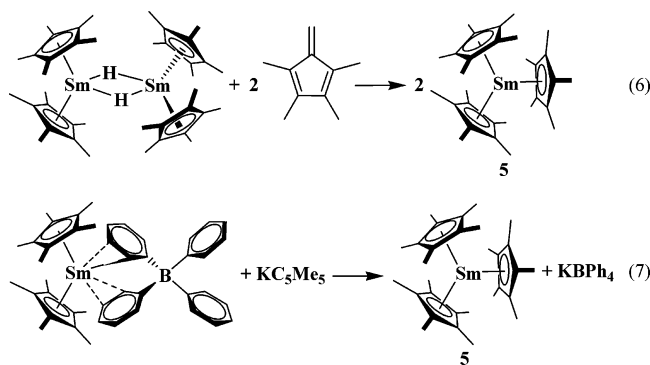
(30) Evans, W. J. *J. Organomet. Chem.* **2002**, *647*, 2.

(31) Bochkarev, M. N. *Coord. Chem. Rev.* **2004**, *248*, 835.

left the components $(C_5Me_5)^-$ and $[(C_5Me_5)_2Sm]^+$. These formed the sterically crowded $(C_5Me_5)_3Sm$ because there was no better alternative.¹ The next synthesis discovered for $(C_5Me_5)_3Sm$, eq 5,³² used a similar strategy in which Pb metal was the stable product that formed also leaving $(C_5Me_5)^-$ and $[(C_5Me_5)_2Sm]^+$.



It was unfortunately not possible to extend these $(C_5Me_5)_3Sm$ synthetic routes to La, Ce, Pr, and Nd, since these metals do not have chemistry analogous to the special reactivity of Sm(II). Syntheses of $(C_5Me_5)_3Sm$ from Sm(III) precursors had to be developed to expand $(C_5Me_5)_3Ln$ chemistry to other metals. As shown in eq 6⁷ and 7,³³ these reactions are based on a similar



approach of making stable byproducts: $(C_5Me_5)^-$ and $KBPh_4$, respectively. $(C_5Me_5)_3Nd$ was readily synthesized in an analogous manner via eq 7,³³ but syntheses of the less crowded complexes of the larger metals proved surprisingly more difficult. To isolate $(C_5Me_5)_3La$, silylated glassware was necessary.³⁴

We now report that $(C_5Me_5)_3Ce$ and $(C_5Me_5)_3Pr$ can be made under the similarly stringent conditions used for the lanthanum analogue. The syntheses of these new $(C_5Me_5)_3Ln$ complexes allowed the stepwise comparison of reactivity vs radial size of the metal for the series $Ln = La-Nd$ and Sm. Presented here are comparisons of the reactivity of this series of complexes using the two known reaction patterns identified for $(C_5Me_5)_3Ln$ complexes, eqs 2 and 3. In the course of these comparisons, several new reactions of $(C_5Me_5)_3Sm$ have been identified as well as a new synthesis of $(C_5Me_5)_3Sm$.

Experimental Section

The syntheses and manipulations of the extremely air- and moisture-sensitive compounds described below were conducted under nitrogen or argon with rigorous exclusion of air and water by Schlenk, vacuum line, and glovebox techniques. Unless specified otherwise, all glovebox manipulations were carried out in an argon-filled glovebox that was free of

coordinating solvents. Glassware was treated with Siliclad (Glest) to avoid formation of oxide decomposition products.

Tetrahydrofuran, diethyl ether, toluene, hexanes, and benzene were saturated with UHP grade argon (Airgas) and dried by passage through Glasscontour drying columns. All deuterio-solvents (Cambridge Isotope Laboratories) were distilled over a NaK alloy and benzophenone and degassed by freeze-pump-thaw cycles (3×). The $(C_5Me_5)_3Ln$ complexes ($Ln = La$, **1**,³⁴ Ce, **2**; Pr, **3**; Nd, **4**,³³ and Sm, **5**³²) were prepared according to the literature or as described below. Due to the high reactivity of the $(C_5Me_5)_3Ln$ complexes, they are synthesized on the scale needed for immediate use in subsequent reaction chemistry. This is typically at the 100 mg level. The precursor cations, $[(C_5Me_5)_2Ln][BPh_4]$, however, can readily be made on the multigram scale. Hydrated lanthanum trichlorides were desolvated with NH_4Cl .³⁵ $(C_5Me_5)_2LnCl_2K(THF)_2$ ³⁶ was synthesized from $LnCl_3$ and KC_5Me_5 from literature methods. KC_5Me_5 ,¹⁶ Et_3NHBPh_4 ,³⁷ $(C_5Me_5)_2$,²³ and $AgBPh_4$ ³⁸ were prepared as previously described. Ph_3PSe (Aldrich) and 2,6- $Ph_2C_6H_3I$ (Aldrich) were placed under vacuum (10^{-3} Torr) for

12 h before use. CH_3I , $C_6H_{11}Br$, and $CH_2CH_2CHCH_2Br$, bromomethylcyclopropane, were purchased from Aldrich and vacuum distilled prior to use. Phenazine and I_2 were purchased from Aldrich and sublimed prior to use. C_6H_5X ($X = F, Cl, Br, I$) (Aldrich) and C_6D_5Cl (Cambridge Isotopes) were dried over Type 4 molecular sieves and degassed by freeze-pump-thaw cycles (3×) before use. C_8H_8 (Aldrich) was distilled, dried over Type 4 molecular sieves, and degassed by freeze-pump-thaw cycles (3×). Ultrahigh-purity CO (Airgas) was passed through a microporous fiberglass purification column (Airgas). Research grade H_2 , CO_2 , C_2H_4 (Airgas) and $(C_3H_5)MgCl$ (2.0 M in THF, Aldrich) were used as received. 1H and ^{13}C NMR spectra were obtained on a Bruker DRX 400 MHz or Omega 500 MHz at 25 °C. Infrared analyses were acquired as thin films from alkanes or arenes using an Applied Systems ReactIR 1000.³⁹ Elemental analyses were performed by Analytische Laboratorien, Lindlar (Germany), or by complexometric titration.⁴⁰

$(C_5Me_5)_3Ce$, **2.** In a nitrogen-filled glovebox that contained coordinating solvents, a solution of $(C_3H_5)MgCl$ (1.1 mL, 2.2 mmol) in THF was added to a yellow solution of $(C_5Me_5)_2CeCl_2K(THF)_2$ (1.404 g, 2.1 mmol) in THF (50 mL). Over 3 h, the solution became green-yellow and a white precipitate formed. After centrifugation, the solvent was removed by rotary evaporation. Extraction of the solvent with 10:1 hexane/dioxane generated additional precipitate that was removed by centrifugation. Removal of solvent gave $(C_5Me_5)_2Ce(C_3H_5)(THF)$ as a yellow powder. 1H NMR (C_6D_6): δ 5.7 (s, 1H, C_3H_5), 2.8 (br s, 30 H, C_5Me_5), -16.5 (s, 2H, C_3H_5), -18.9 (s, 2H, C_3H_5). $(C_5Me_5)_2Ce(C_3H_5)(THF)$ was transferred into a sublimation tube equipped with a sealable Teflon adapter, and $(C_5Me_5)_2Ce(C_3H_5)(THF)$ was desolvated by exposure to vacuum (1×10^{-5} Torr) for 24 h followed by an additional day at 60 °C. The apparatus was brought into an argon-filled glovebox that was free of coordinating solvents. Extraction into hexanes and rotary evaporation provided $(C_5Me_5)_2Ce(C_3H_5)$ (0.607 g, 64%) as a bright green powder. 1H NMR (C_6D_6 , 20 °C): δ 16.2 (s, 1H, C_3H_5), 2.5 (d, 30H, C_5Me_5), -16.6 (s, 2H, C_3H_5), -24.3 (s, 2H, C_3H_5). ^{13}C NMR (C_6D_6): δ 102.4 (C_5Me_5), 31.9, 23.0 (C_3H_5), 14.3 (C_5Me_5). IR: 2957s, 2910s, 2856s, 2725w, 1441m, 1378m, 1262s, 1092s, 1019s, 803m, 694w cm^{-1} . Anal. Calcd for

(35) Taylor, M. D.; Carter, C. P. *J. Inorg. Nucl. Chem.* **1962**, *24*, 387.

(36) Evans, W. J.; Keyer, R. A.; Ziller, J. W. *Organometallics* **1993**, *12*, 2618.

(37) Evans, W. J.; Johnston, M. A.; Greci, M. A.; Gummshheimer, T. S.; Ziller, J. W. *Polyhedron* **2003**, *22*, 119.

(38) Jordan, R. F.; Echols, S. F. *Inorg. Chem.* **1987**, *26*, 383

(39) Evans, W. J.; Johnston, M. A.; Clark, R. D.; Ziller, J. W. *Inorg. Chem.* **2000**, *39*, 3421.

(40) Atwood, J. L.; Hunter, W. E.; Wayda, A. L.; Evans, W. J. *Inorg. Chem.* **1981**, *20*, 4115.

(32) Evans, W. J.; Forrestal, K. J.; Leman, J. T.; Ziller, J. W. *Organometallics* **1996**, *15*, 527.

(33) Evans, W. J.; Seibel, C. A.; Ziller, J. W. *J. Am. Chem. Soc.* **1998**, *120*, 6745.

(34) Evans, W. J.; Davis, B. L.; Ziller, J. W. *Inorg. Chem.* **2001**, *40*, 6341.

$CeC_{23}H_{35}$: Ce, 31.0. Found: Ce, 30.6. Addition of $(C_5Me_5)_2Ce$ - (C_3H_5) (0.792 g, 2.5 mmol) to Et_3NHBPh_4 (1.16 g, 2.8 mmol) in benzene (6 mL) produced a green slurry, which became pink within 12 h. Removal of gray insoluble materials by centrifugation afforded a bright pink solution. The solvent was removed via rotary evaporation to leave $[(C_5Me_5)_2Ce][BPh_4]$ as a bright pink powder (1.71 g, 94%). 1H NMR (C_6D_6 , 40 °C): δ 6.3 (br s, C_5Me_5). The $(BPh_4)^-$ resonances were not located. IR: 2957s, 2926s, 2860m, 1857w, 1810w, 1606m, 1498m, 1463s, 1378s, 1247w, 1154w, 1081w, 1031s, 891w, 845w, 725m, 675s cm^{-1} . Anal. Calcd for $CeBC_{44}H_{50}$: Ce, 19.2. Found: Ce, 19.1.

$[(C_5Me_5)_2Ce][BPh_4]$ was recrystallized as pink needles from hot toluene (100 mg in 17 mL) by slow cooling to -35 °C. The crystalline $[(C_5Me_5)_2Ce][BPh_4]$ was washed three times with hexane and dried under vacuum before use. In a silylated glass vial, $[(C_5Me_5)_2Ce][BPh_4]$ (0.064 g, 0.088 mmol) was combined with KC_5Me_5 (0.017 g, 0.098 mmol) in benzene (5 mL) to give a pink slurry, which was stirred for 24 h. This resulted in a green slurry, from which gray insoluble solids were removed via centrifugation. The solvent was removed from the resulting green supernatant to leave **2** as a green powder (45 mg, 94%). The overall yield from $CeCl_3$ is 57%. 1H NMR (C_6D_6 , 20 °C): δ 3.2 (br s, 45H, C_5Me_5 , $\Delta\nu_{1/2} = 50$ Hz). ^{13}C NMR: δ 174.6 (C_5Me_5), 8.0 (C_5Me_5). IR: 2957 m, 2922s, 2142w, 1853w, 1459s, 1378s, 1262m, 1185w, 1154m, 1080w, 1031m, 907w, 745m cm^{-1} . Anal. Calcd for $CeC_{30}H_{45}$: Ce, 25.7. Found: Ce, 25.9. Green crystals of **2** suitable for X-ray analysis formed from a concentrated toluene solution at -35 °C. Failure to use silylated glassware or recrystallized $[(C_5Me_5)_2Ce][BPh_4]$ resulted in the formation of large amounts of $[(C_5Me_5)_2Ce]_2(\mu-O)$; 1H NMR (C_6D_6) 1.9 ppm; the unit cell constants, $a = b = 11.466$ Å, $c = 14.210$ Å; $\alpha = \beta = \gamma = 90^\circ$, match those of other $[(C_5Me_5)_2Ln]_2(\mu-O)$ complexes.^{41–44}

$(C_5Me_5)_3Pr$, **3**. As described above in the synthesis of **2**, a solution of $(C_3H_5)MgCl$ (2.5 mL, 5.00 mmol) in THF was reacted with a green solution of $(C_5Me_5)_2PrCl_2K(THF)_2$ (3.106 g, 4.96 mmol) in THF (50 mL) to form $(C_5Me_5)_2Pr(C_3H_5)(THF)$ as a yellow powder. $(C_5Me_5)_2Pr(C_3H_5)(THF)$ was desolvated, and $(C_5Me_5)_2Pr(C_3H_5)$ (1.173 g, 52%) was isolated as a yellow powder. 1H NMR (C_6D_6): δ 5.6 (s, 15H, C_5Me_5 , $\Delta\nu_{1/2} = 25$ Hz), 4.5 (s, 15H, C_5Me_5 , $\Delta\nu_{1/2} = 25$ Hz). Only $(C_5Me_5)^-$ methyl resonances were located.⁴⁵ $(C_5Me_5)_2Pr(C_3H_5)$ (1.183 g, 2.62 mmol) and Et_3NHBPh_4 (1.157 g, 2.75 mmol) were combined in benzene (10 mL), and $[(C_5Me_5)_2Pr][BPh_4]$ (1.779 g, 93%) was isolated as a yellow powder. 1H NMR (C_6D_6): δ 14.7 (br s, 30H, C_5Me_5 , $\Delta\nu_{1/2} = 265$ Hz). The $(BPh_4)^-$ resonances were not located. Anal. Calcd for $PrBC_{44}H_{50}$: Pr, 19.3. Found: Pr, 19.5.

Freshly recrystallized $[(C_5Me_5)_2Pr][BPh_4]$ (134 mg, 0.184 mmol) was reacted with KC_5Me_5 (43 mg, 0.249 mmol) in benzene (10 mL) to form $(C_5Me_5)_3Pr$ as a dark yellow powder (98 mg, 98%). The overall yield from $PrCl_3$ is 47%. 1H NMR (C_6D_6): δ 6.8 (s, 45H, C_5Me_5 , $\Delta\nu_{1/2} = 10$ Hz). ^{13}C NMR (C_6D_6): δ -3.4 (C_5Me_5), 279 (C_5Me_5), assignments confirmed by HMQC. IR: 3057m, 2964s, 3910s, 2860s, 2729w, 1606s, 1583m, 1478s, 1428s, 1378s, 1262s, 1185m, 1150m, 1081s, 1031s, 918m, 849m, 733s, 706s cm^{-1} . Anal. Calcd for $PrC_{30}H_{45}$: Pr, 25.8. Found: Pr, 25.4. Crystals of **3** suitable for X-ray analysis formed from a hot toluene solution slowly cooled to -35 °C overnight. Failure to use silylated glassware or recrystallized $[(C_5Me_5)_2Pr][BPh_4]$ results in the formation of large amounts of $[(C_5Me_5)_2Pr]_2(\mu-O)$; 1H NMR (C_6D_6) δ 2.9 (s, 30H, C_5Me_5 , $\Delta\nu_{1/2} = 10$ Hz); unit cell constants, $a = 11.466$ Å, $b = 11.466$

Å, $c = 14.210$ Å; $\alpha = \beta = \gamma = 90^\circ$, match those of other $[(C_5Me_5)_2Ln]_2(\mu-O)$ complexes.^{41–44}

$(C_5Me_5)_3Sm$, **5**, from $(C_5Me_5)_2Sm$ and $(C_5Me_5)_2$. Dark green $(C_5Me_5)_2Sm$ (73 mg, 0.173 mmol) and $(C_5Me_5)_2$ ⁴⁶ (23 mg, 0.087 mmol) were combined in a flask and dissolved in benzene (20 mL). Although no reaction was observed by 1H NMR spectroscopy after 24 h at 25 °C, heating the reaction mixture at 80 °C for 2 h turned the solution from dark green to dark brown. The 1H NMR spectrum revealed complete disappearance of $(C_5Me_5)_2Sm$ and $(C_5Me_5)_2$ with the formation of $(C_5Me_5)_3Sm$.¹ Removal of the solvent left $(C_5Me_5)_3Sm$ as a brown solid (40 mg, 84%).

Reactivity of $(C_5Me_5)_3Ln$. Representative examples are given with each substrate.

With CO. $(C_5Me_5)_2Ce(O_2C_7Me_5)$. A solution of $(C_5Me_5)_2Ce$ (0.131 g, 0.24 mmol) in toluene (20 mL) in a round-bottom flask was degassed by freeze–pump–thaw cycles (3 \times) on a vacuum line. CO (1 atm) was introduced and after 24 h the color changed from bright green to brown-pink. Removal of solvent afforded $(C_5Me_5)_2Ce(O_2C_7Me_5)$ (0.121 g, 87%). 1H NMR (C_6D_6 , 20 °C): δ 5.6 (s, 3H, $O_2C_7Me_5$), 2.4 (s, 15H, C_5Me_5), 2.3 (s, 6H, $O_2C_7Me_5$), 2.2 (s, 15H, C_5Me_5), -0.6 (s, 6H, $O_2C_7Me_5$). IR: 2964s, 2914m, 2856m, 1652w, 1540s, 1440s, 1378m, 1262s, 1085s, 1065s, 1019s, 930w, 799m, 710m cm^{-1} . For comparison, $(C_5Me_5)_2Nd(O_2C_7Me_5)$ ³³ has the following IR: 2964s, 2902s, 2851s, 1533s, 1441s, 1402w, 1370s, 1302w, 1107m, 1066w, 1015w, 974w, 723w, 692w, 635w cm^{-1} .

$(C_5Me_5)_2Pr(O_2C_7Me_5)$. Following the procedure above, $(C_5Me_5)_2Pr$ (63 mg, 0.115 mmol) was reacted with CO (1 atm) in toluene (10 mL) to form yellow $(C_5Me_5)_2Pr(O_2C_7Me_5)$ (52 mg, 81%). 1H NMR (C_6H_6 , 20 °C): δ 6.1 (s, 15H, $\Delta\nu_{1/2} = 9$ Hz, C_5Me_5), 5.4 (s, 15H, $\Delta\nu_{1/2} = 9$ Hz, C_5Me_5), 2.7 (s, 3H, $\Delta\nu_{1/2} = 9$ Hz, $O_2C_7Me_5$), 1.0 (s, 6H, $\Delta\nu_{1/2} = 3$ Hz, $O_2C_7Me_5$), -12.7 (s, 6H, $\Delta\nu_{1/2} = 6$ Hz, $O_2C_7Me_5$). IR: 2968m, 2910s, 2856s, 2729w, 1532s, 1478m, 1444m, 1401m, 1366m, 1305w, 1262w, 1108m, 1069w, 1034w, 976w, 799w, 741m, 706m, 649m cm^{-1} .

$(C_5Me_5)_2La(O_2C_7Me_5)$. A solution of $(C_5Me_5)_3La$ in C_6D_6 in a J-Young NMR tube was degassed as described for $(C_5Me_5)_2Ce(O_2C_7Me_5)$. CO (1 atm) was introduced into the tube, and after 3 days at room temperature, resonances started to appear in the 1H NMR spectrum. After several days at 50 °C the starting material was consumed and a new set of peaks consistent with those of the $(C_5Me_5)_2Ln(O_2C_7Me_5)$ complexes of Ce, Pr, Nd,¹³ and Sm⁶ was observed: 1H (C_6D_6) δ 2.04 (s, 15H, C_5Me_5), 1.99 (s, 15H, C_5Me_5), 1.49 (s, 6H, $O_2C_7Me_5$), 1.13 (s, 6H, $O_2C_7Me_5$), 1.11 (s, 3H, $O_2C_7Me_5$).

With C_2H_4 . A solution of $(C_5Me_5)_3Nd$ (46 mg, 0.086 mmol) in toluene (25 mL) in a round-bottom flask was attached to a high-vacuum line and degassed by freeze–pump–thaw cycles (3 \times). Ethylene (1 atm) was introduced into the flask. Polymer precipitation occurred within 5 min, and after 20 min the solution was too viscous to stir. After approximately an hour, the reaction was quenched with methanol and washed with acidic water. The polymer was dried under high vacuum for 8 h (0.035 g). Under similar conditions, $(C_5Me_5)_3Ce$ (0.038 g, 0.07 mmol) generated 0.09 g of polymer, but formation of the insoluble polymer was not observed until 1 h after addition of monomer. The polymer was too insoluble to obtain NMR spectra.^{47,48}

With H_2 . A solution of $(C_5Me_5)_3Nd$ (20 mg, 0.036 mmol) in C_6D_6 (1 mL) in a J-Young NMR tube was degassed on a high-vacuum line by freeze–pump–thaw cycles (3 \times). H_2 (1 atm)

(41) Evans, W. J.; Grate, J. W.; Bloom, I.; Hunter, W. E.; Atwood, J. L. *J. Am. Chem. Soc.* **1985**, *107*, 405.

(42) Tilley, T. D.; Rheingold, A. L.; Allen, M. B. Personal Communication to Cambridge Structure Database, 1996.

(43) Ringelberg, S. N.; Meetsma, A.; Troyanov, S. I.; Hessen, B.; Teuben, J. H. *Organometallics* **2002**, *21*, 1759.

(44) Evans, W. J.; Davis, B. L.; Nyce, G. W.; Perotti, J. M.; Ziller, J. W. *J. Organomet. Chem.* **2003**, *677*, 89.

(45) Evans, W. J.; Kozimor, S. A.; Brady, J. C.; Davis, B. L.; Nyce, G. W.; Seibel, C. A.; Ziller, J. W.; Doedens, R. J. *Organometallics* **2005**, *24*, 2269.

(46) Culshaw, P. N.; Walton, J. C.; Hughes, L.; Ingold, K. U. *J. Chem. Soc., Perkin Trans. 2* **1993**, 879.

(47) Evans, W. J.; DeCoster, D. M.; Greaves, J. *Macromolecules* **1995**, *28*, 7929.

(48) Evans, W. J.; DeCoster, D. M.; Greaves, J. *Organometallics* **1996**, *15*, 3210.

was introduced into the NMR tube, and after 4 days a blue-green precipitate had formed. The ^1H NMR spectrum was consistent with the formation of $[(\text{C}_5\text{Me}_5)_2\text{NdH}]_x$ ^{49,50} and $\text{C}_5\text{Me}_5\text{H}$.

With $\text{Ph}_3\text{P}=\text{Se}$. Following the synthesis of $[(\text{C}_5\text{Me}_5)_2\text{Nd}]_2(\mu-\eta^2:\eta^2-\text{Se}_2)$,¹⁰ $(\text{C}_5\text{Me}_5)_3\text{La}$ (0.147 g, 0.272 mmol) was reacted with $\text{Ph}_3\text{P}=\text{Se}$ (0.092 g, 0.272 mmol) for 17 h in toluene (10 mL) to give $[(\text{C}_5\text{Me}_5)_2\text{La}]_2(\mu-\eta^2:\eta^2-\text{Se}_2)$, **6**, isolated as a red solid. **6** was washed with toluene to remove Ph_3P and isolated in 81% yield (0.107 g). ^1H NMR (C_6D_6 , 350 K): δ 2.17. ^{13}C NMR (C_6D_6): δ 122.1, 11.6. Crystals of **6** suitable for X-ray analysis formed from a hot toluene solution, and recrystallization of **6** from toluene/THF formed $[(\text{C}_5\text{Me}_5)_2\text{La}(\text{THF})]_2(\mu-\eta^2:\eta^2-\text{Se}_2)$, **7**.

With AgBPh_4 . AgBPh_4 (41 mg, 0.096 mmol) was added to a flask that had been wrapped in aluminum foil and charged with a solution of $(\text{C}_5\text{Me}_5)_3\text{Nd}$ (53 mg, 0.096 mmol) in toluene (5 mL). After the reaction was stirred for 8 h, a gray precipitate was removed by centrifugation and the solvent was removed by rotary evaporation to yield a tacky green solid. The solid was washed with hexanes and dried under vacuum to yield $[(\text{C}_5\text{Me}_5)_2\text{Nd}][\text{BPh}_4]$ ³³ (52 mg, 75%), identified by ^1H NMR spectroscopy. The hexane washings were collected in a vial, and the solvent was removed by rotary evaporation to yield $(\text{C}_5\text{Me}_5)_2$ as a yellow oil identified by ^1H NMR spectroscopy.²³

As described above, $(\text{C}_5\text{Me}_5)_3\text{Ce}$ (0.045 g, 0.08 mmol) was reacted with AgBPh_4 (0.036 g, 0.09 mmol) in benzene (5 mL). $(\text{C}_5\text{Me}_5)_2$ and the pink $[(\text{C}_5\text{Me}_5)_2\text{Ce}][\text{BPh}_4]$ were identified by NMR (0.054 g, 89%).

With Phenazine. $(\text{C}_5\text{Me}_5)_3\text{Sm}$ (30 mg, 0.054 mmol) was combined with phenazine (5 mg, 0.027 mmol) in toluene (5 mL) and stirred for 12 h. The solvent was removed in vacuo, and the black-brown solids were dissolved in C_6D_6 . ^1H NMR spectroscopy indicated exclusive formation of $[(\text{C}_5\text{Me}_5)_2\text{Sm}]_2(\mu-\eta^3:\eta^3-\text{C}_{12}\text{N}_2\text{H}_8)$ ⁵¹ and $(\text{C}_5\text{Me}_5)_2$.²³ Black microcrystals of $[(\text{C}_5\text{Me}_5)_2\text{Sm}]_2(\mu-\eta^3:\eta^3-\text{C}_{12}\text{N}_2\text{H}_8)$ (20 mg, 72%) were separated from $(\text{C}_5\text{Me}_5)_2$ by washing with hexanes (3×5 mL).

As described above for $(\text{C}_5\text{Me}_5)_3\text{Sm}$, $(\text{C}_5\text{Me}_5)_3\text{La}$ (34 mg, 0.062 mmol) reacts with phenazine (6 mg, 0.031 mmol) in toluene to form a deep red solution. After 24 h, the solvent was removed in vacuo to yield a red solid. The ^1H NMR spectrum contained the peaks reported for $[(\text{C}_5\text{Me}_5)_2\text{La}]_2(\mu-\eta^2:\eta^2-\text{C}_{12}\text{N}_2\text{H}_8)$, **8**,⁵² and $(\text{C}_5\text{Me}_5)_2$.²³ X-ray quality crystals grown from hot toluene (23 mg, 75%) confirmed that an identical product had formed. Anal. Calcd for $\text{La}_2\text{C}_{52}\text{H}_{68}\text{N}_2$: La, 13.9. Found: La, 13.3.

With CO_2 . $(\text{C}_5\text{Me}_5)_2\text{Sm}(\text{O}_2\text{CC}_5\text{Me}_5)$, **9**. A brown solution of $(\text{C}_5\text{Me}_5)_3\text{Sm}$ (238 mg, 0.428 mmol) in toluene (25 mL) in a round-bottom flask was degassed by freeze-pump-thaw cycles ($2 \times$) on a vacuum line. CO_2 (1 atm) was introduced into the vessel, and after 1 min the solution changed in color to orange-yellow. The solution was degassed, and the reaction vessel was returned to the glovebox. Solvent was removed by rotary evaporation, and the compound was dried under vacuum to yield $(\text{C}_5\text{Me}_5)_2\text{Sm}(\text{O}_2\text{CC}_5\text{Me}_5)$ as an orange solid (241 mg, 94%). ^1H NMR (C_6D_6): δ 3.6 (s, 3H, $\text{O}_2\text{CC}_5\text{Me}_5$), 3.1 (s, 6H, $\text{O}_2\text{CC}_5\text{Me}_5$), 2.4 (s, 6H, $\text{O}_2\text{CC}_5\text{Me}_5$), 0.7 (s, 30H, C_5Me_5). ^{13}C NMR (C_6D_6): δ 12.2, 13.4, 17.7, 22.4, 67.5, 115.0, 119.2, 137.8, 140.6. IR 2964s, 2914s, 2856s, 2737w, 2281w, 1660w, 1552s, 1440s, 1397s, 1355s, 1262s, 1085s, 1015s, 922m, 803s, 718s, 680s cm^{-1} . Crystals of **9** suitable for X-ray crystallographic analysis were obtained by cooling a toluene solution at -40 $^\circ\text{C}$.

$(\text{C}_5\text{Me}_5)_2\text{Nd}(\text{O}_2\text{CC}_5\text{Me}_5)$. An olive green solution of $(\text{C}_5\text{Me}_5)_3\text{Nd}$ (40 mg, 0.073 mmol) in C_6H_6 (10 mL) was reacted with CO_2 (1 atm) as described above for **9**. $(\text{C}_5\text{Me}_5)_2\text{Nd}$

$(\text{O}_2\text{CC}_5\text{Me}_5)$ was isolated as a light blue-green powder (43 mg, 99%). ^1H NMR (C_6D_6): δ 6.3(s, 30H, C_5Me_5), 1.0 (s, 6H, $\text{O}_2\text{CC}_5\text{Me}_5$), -1.0 (s, 6H, $\text{O}_2\text{CC}_5\text{Me}_5$), -1.4 (s, 3H, $\text{O}_2\text{CC}_5\text{Me}_5$). ^{13}C NMR (C_6D_6): δ -14.3 , 8.4, 10.3, 11.2, 131.5, 133.2, 134.7, 138.9, 293.8. IR 2961s, 2922s, 2856s, 1548vs, 1440m, 1401m, 1378m, 1355s, 1262s, 1081vs, 1065vs, 1023vs, 919w, 802s, 702m cm^{-1} .

With $\text{Et}_3\text{NHBPh}_4$. $(\text{C}_5\text{Me}_5)_3\text{Nd}$ (40 mg, 0.073 mmol) and $\text{Et}_3\text{NHBPh}_4$ (31 mg, 0.073 mmol) were combined in benzene (5 mL) and stirred for 8 h. The solvent was then removed by rotary evaporation, and the solids were washed with hexanes to yield $[(\text{C}_5\text{Me}_5)_2\text{Nd}][\text{BPh}_4]$ (45 mg, 85%), identified by ^1H NMR spectroscopy.³³ The hexane washings were collected in a vial, and the solvent was removed by rotary evaporation to yield $\text{C}_5\text{Me}_5\text{H}$ as a yellow oil identified by ^1H NMR spectroscopy.²³

An orange solution of $(\text{C}_5\text{Me}_5)_3\text{Pr}$ (0.009 g, 0.017 mmol) in benzene (1 mL) was added to $\text{Et}_3\text{NHBPh}_4$ (0.007 g, 0.017 mmol), and the mixture was stirred. The color slowly changed to lemon yellow, and the insoluble $\text{Et}_3\text{NHBPh}_4$ was consumed. After 3 h the solution was centrifuged to remove any unreacted $\text{Et}_3\text{NHBPh}_4$, and ^1H NMR spectroscopy (C_6H_6 , No-D NMR) showed complete consumption of $(\text{C}_5\text{Me}_5)_3\text{Pr}$ and formation of $[(\text{C}_5\text{Me}_5)_2\text{Pr}][\text{BPh}_4]$, $\text{C}_5\text{Me}_5\text{H}$, and NEt_3 . This No-D ^1H NMR experiment was conducted as previously described.⁵³

Reaction of $(\text{C}_5\text{Me}_5)_3\text{Sm}$ and Bromomethylcyclopropane. A sample of $\text{CH}_2\text{CH}_2\text{CHCH}_2\text{Br}$ (4.2 μL , 0.043 mmol) chilled to -38 $^\circ\text{C}$ in a glovebox refrigerator was added to a dark brown solution of $(\text{C}_5\text{Me}_5)_3\text{Sm}$ (20 mg, 0.036 mmol) in C_6D_6 (1 mL) in a J-Young NMR tube. Red-brown solids precipitated immediately. The ^1H NMR spectrum as well as the GC-MS analysis of the deuterolyzed products matched that of the $(\text{CH}_2\text{CH}_2\text{CH})\text{CH}_2(\text{C}_5\text{Me}_5)$ and $\text{CH}_2=\text{CHCH}_2\text{CH}_2\text{C}_5\text{Me}_5$ ⁵⁴ standards, which were independently prepared from KC_5Me_5 and $\text{CH}_2\text{CH}_2\text{CHCH}_2\text{Br}$ and $\text{CH}_2=\text{CHCH}_2\text{CH}_2\text{Br}$, respectively.

The $(\text{CH}_2\text{CH}_2\text{CH})\text{CH}_2(\text{C}_5\text{Me}_5)$ to $\text{CH}_2=\text{CHCH}_2\text{CH}_2\text{C}_5\text{Me}_5$ ⁵⁴ ratio was 74:26. In addition to these RC_5Me_5 products, the ^1H NMR spectrum of the crude reaction mixture contained three singlets of equal intensity at δ 0.99, 0.53, and -0.85 that may be attributed to $(\text{C}_5\text{Me}_5)^-$ ligands attached to samarium. A similar pattern was observed in the reduction products of alkyl chlorides by $(\text{C}_5\text{Me}_5)_2\text{Sm}(\text{OEt}_2)$,⁵⁵ and this was attributed to $[(\text{C}_5\text{Me}_5)_3\text{Sm}_2\text{Cl}_3]_x$. In this case, the resonances could arise from a bromide analogue.

Reaction of $(\text{C}_5\text{Me}_5)_3\text{Sm}$ and 6-Bromo-1-hexene. Slow addition of cold $\text{C}_6\text{H}_{11}\text{Br}$ (2.2 μL , 0.016 mmol) to a solution of $(\text{C}_5\text{Me}_5)_3\text{Sm}$ (9.0 mg, 0.016 mmol) in C_6D_6 (1 mL) in a J-Young NMR tube caused red-brown solids to precipitate immediately as described above. The ^1H NMR spectrum contained the same three C_5Me_5 resonances found above in addition to a broad singlet at δ 0.41. Only one RC_5Me_5 species, the 5-hexenyl- C_5Me_5 ($\text{C}_5\text{Me}_5\text{C}_6\text{H}_{11}$), was discernible via NMR. A GC-MS of the solution revealed one major species with $m/z = 218$, in addition to another with the same mass formed in a much smaller quantity ($<4\%$ relative to the former). The identity of the $\text{C}_5\text{Me}_5\text{C}_6\text{H}_{11}$ was confirmed by a comparison with the authentic product made independently from KC_5Me_5 and $\text{C}_6\text{H}_{11}\text{Br}$ in C_6D_6 . ^1H NMR (C_6D_6): δ 5.73 (m, 1H, $\text{H}_2\text{C}=\text{CH}$), 4.95 (m, 2H, $\text{H}_2\text{C}=\text{CH}$), 1.92 (m, 2H, $\text{H}_2\text{CCH}(\text{CH}_2)_4$), 1.74 (s, 6H, C_5Me_5), 1.69 (s, 6H, C_5Me_5), 1.38 (m, 2H $\text{H}_2\text{CCH}(\text{CH}_2)_4$), 1.26 (m, 2H, $\text{H}_2\text{CCH}(\text{CH}_2)_4$), 0.93 (s, 3H, C_5Me_5), 0.76 (m, 2H,

(49) Scholz, J.; Scholz, A.; Weimann, R.; Janiak, C.; Schumann, H. *Angew. Chem., Int. Ed. Engl.* **1994**, *33*, 1171.

(50) Hoye, T. R.; Eklöv, B. M.; Ryba, T. D.; Voloshin, M.; Yao, L. J. *Org. Lett.* **2004**, *6*, 953.

(51) Finke, R. G.; Keenan, S. R.; Watson, P. L. *Organometallics* **1989**, *8*, 263.

(52) Finke, R. G.; Keenan, S. R.; Schiraldi, D. A.; Watson, P. L. *Organometallics* **1987**, *6*, 1356.

(49) Jeske, G.; Lauke, H.; Mauermann, H.; Swepston, P. N.; Schumann, H.; Marks, T. J. *J. Am. Chem. Soc.* **1985**, *107*, 8091.

(50) Heeres, H. J.; Renkema, J.; Booi, M.; Meetsma, A.; Teuben, J. H. *Organometallics* **1988**, *7*, 2495.

(51) Evans, W. J.; Gonzales, S. L.; Ziller, J. W. *J. Am. Chem. Soc.* **1994**, *116*, 2600.

Table 1. Experimental Data from the X-ray Diffraction Studies of (C₅Me₅)₃Ce, **2, (C₅Me₅)₃Pr, **3**, [(C₅Me₅)₂La]₂(μ-η²:η²-Se₂), **6**, [(C₅Me₅)₂La(THF)]₂(μ-η²:η²-Se₂), **7**, [(C₅Me₅)₂La]₂(μ-η³:η³-C₁₂N₂H₈), **8**, (C₅Me₅)₂Sm(O₂CC₅Me₅), **9**, and [(C₅Me₅)₂Sm(μ-I)]₃, **10****

	2	3	6	7	8	9	10
formula	C ₃₀ H ₄₅ Ce	C ₃₀ H ₄₅ Pr	C ₄₀ H ₆₀ La ₂ Se ₂	C ₄₈ H ₇₆ La ₂ O ₂ Se ₂ ·2(C ₇ H ₈)	C ₅₂ H ₆₈ La ₂ N ₂ ·C ₆ H ₆	C ₃₁ H ₄₅ O ₂ Sm	C ₆₀ H ₉₀ I ₃ Sm ₃
fw	545.78	546.57	976.62	1305.10	1077.01	600.02	1643.07
temp (K)	178(2)	158(2)	193(2)	158(2)	163(2)	158(2)	158(2)
space group	<i>P6₃/m</i>	<i>P6₃/m</i>	<i>P2₁/n</i>	<i>P1</i>	<i>P1</i>	<i>C2/c</i>	<i>C2/c</i>
<i>a</i> (Å)	10.070(4)	10.0310(4)	8.5697(11)	10.4164(6)	10.5137(3)	38.1766(18)	21.9414(13)
<i>b</i> (Å)	10.070(4)	10.0310(4)	20.622(3)	10.8623(6)	11.2006(4)	10.1681(5)	14.3377(9)
<i>c</i> (Å)	15.5383(8)	15.5223(7)	11.8095(15)	13.2748(8)	11.3252(4)	15.7555(8)	20.4157(12)
α (deg)	90	90	90	80.9350(10)	80.6170(10)	90	90
β (deg)	90	90	102.427(2)	83.4830(10)	76.6950(10)	109.1230(10)	107.9360(10)
γ (deg)	120	120	90	83.9480(10)	80.6170(10)	90	90
<i>V</i> (Å ³)	1364.70(10)	1352.62(10)	2038.1(4)	1467.77(15)	1280.38(7)	5778.5(5)	6110.4(6)
<i>Z</i>	2	2	2	1	1	8	4
<i>D</i> _{calcd} (Mg/m ³)	1.328	1.342	1.591	1.477	1.397	1.379	1.786
μ (mm ⁻¹)	1.681	1.815	3.878	2.715	1.683	2.056	4.395
final <i>R</i> indices	0.0163	0.0217	0.0701	0.0348	0.0260	0.0404	0.0278
[<i>I</i> > 2σ(<i>I</i>)]							
wR2 (all data)	0.0422	0.0631	0.1695	0.0910	0.0648	0.0877	0.0747

H₂CCH(CH₂)₄. MS mass calcd for C₅Me₅C₆H₁₁: *m/z* = 218. Found: *m/z* = 218.

Reaction of (C₅Me₅)₃Sm and Phenyl Iodide. Cold C₆H₅I (6.0 μL, 0.054 mmol) was added slowly to a solution of (C₅Me₅)₃Sm (30 mg, 0.054 mmol) in C₆D₆ (1 mL) in a silylated J-Young tube in the absence of light. Dark red solids precipitate from the reaction mixture within 6 h. The ¹H NMR spectrum of this product contains resonances for (C₆H₅)₂, (C₅Me₅)₂, C₅Me₅(C₆H₅), and C₅Me₅I in addition to [(C₅Me₅)₂Sm(μ-I)]₃. Analysis of the reaction supernatant via GC-MS shows the following: *m/z* = 154 (MS calcd for (C₆H₅)₂: *m/z* = 154), *m/z* = 212 (MS calcd for C₅Me₅(C₆H₅): *m/z* = 212), and *m/z* = 170 (MS calcd for C₅Me₅I: *m/z* = 170). The dark red precipitate was collected from the supernatant via centrifuge, the red powder was dried under vacuum, and [(C₅Me₅)₂Sm(μ-I)]₃, **10** (25 mg, 86%), was isolated as a red powder. ¹H NMR (C₆D₆): δ 0.66 (s, C₅Me₅). Calcd for SmI₂C₂₀H₃₀: Sm, 27.46; I, 23.17; C 43.85; H, 5.52. Found: Sm, 27.70; I, 23.39; C, 43.58; H, 5.28.

[(C₅Me₅)₂Sm(μ-I)]₃, **10, from (C₅Me₅)₃Sm and I₂.** (C₅Me₅)₃Sm (40 mg, 0.072 mmol) in toluene (12 mL) was placed in one side of an H-shaped apparatus comprised of 10 mm glass tubing. The middle of the H contains a coarse frit. The tops of the sides of the H are capped with grease-free high-vacuum stopcocks whose outlets connect to each other through a tube parallel to the tube comprising the middle of the H. This upper tube is connected to a 24/40 adapter. Under a strong purge of nitrogen, the stopcock on the other side of the H tube was removed and solid I₂ (10 mg, 0.039 mmol) was added. The entire apparatus was evacuated to the pressure of the solvent, and iodine vapor was allowed to diffuse into the (C₅Me₅)₃Sm solution. After 24 h, the solution had changed from brown to purple, and red crystals of **10** whose NMR matched that above were isolated.

Reaction of (C₅Me₅)₃Sm and Terphenyl Iodide (2,6-Ph₂C₆H₃I). (C₅Me₅)₃Sm (8.0 mg, 0.014 mmol) and 2,6-Ph₂C₆H₃I (6.0 mg, 0.017 mmol) were dissolved in C₆D₆ (1 mL) in an NMR tube, which was then sealed under vacuum (10⁻³ Torr). No immediate reaction was observed by ¹H NMR spectroscopy, but after 3 days at room temperature, 86% of the (C₅Me₅)₃Sm was consumed and resonances for (C₅Me₅)₂, C₅Me₅I, and [(C₅Me₅)₂Sm(μ-I)]₃ were found in the ¹H NMR spectrum.

Reaction of (C₅Me₅)₃Sm and Chlorobenzene-*d*₅ (C₆D₅Cl). C₆D₅Cl (3.6 μL, 0.040 mmol) chilled to -35 °C in a glovebox freezer was added slowly to a solution of (C₅Me₅)₃Sm (20 mg, 0.036 mmol) in C₆D₆ (1 mL) in an NMR tube. The NMR tube was flame sealed under vacuum immediately after mixing. The ¹H NMR spectrum showed a 1:1 mixture of (C₅Me₅)₃Sm and [(C₅Me₅)₂Sm(μ-Cl)]₃ after 24 h at room temperature. In addition,

resonances for C₅Me₅(C₆D₅), (C₅Me₅)₂, and C₅Me₅Cl were found in the spectrum. When the NMR tube was heated at 75 °C for 2 h, red solids precipitated. Removal of the supernatant via centrifuge yielded red microcrystalline solids that were identified as [(C₅Me₅)₂Sm(μ-Cl)]₃⁵⁶ (15 mg, 91%). Analysis of the supernatant by GC-MS revealed *m/z* 164 consistent with (C₆D₅)₂, *m/z* 170 consistent with C₅Me₅I, and *m/z* 217 consistent with C₅Me₅(C₆D₅).

X-ray Data Collection, Structure Determination, and Refinement. (C₅Me₅)₃Ce, **2**. A green crystal of approximate dimensions 0.10 × 0.12 × 0.20 mm was mounted on a glass fiber and transferred to a Bruker CCD platform diffractometer. The SMART⁵⁷ program package was used to determine the unit-cell parameters and for data collection (25 s/frame scan time for a sphere of diffraction data). The raw frame data were processed using SAINT⁵⁸ and SADABS⁵⁹ to yield the reflection data file. Subsequent calculations were carried out using the SHELXTL⁶⁰ program. Full details are given in Table 1. The systematic absences were consistent with the hexagonal space groups *P6₃* and *P6₃/m*. It was later determined that the centrosymmetric space group *P6₃/m* was correct.

The structure was solved by direct methods and refined on *F*² by full-matrix least-squares techniques. The analytical scattering factors⁶¹ for neutral atoms were used throughout the analysis. The molecule was located on a site of $\bar{6}$ symmetry. Hydrogen atoms were initially included using a riding model. Subsequent refinement was done with hydrogen *U*_{iso} values riding on the attached methyl carbon and *x*, *y*, *z* free. At convergence, wR2 = 0.0422 and GOF = 1.166 for 78 variables refined against 1177 unique data. As a comparison for refinement on *F*, R1 = 0.0163 for those 1079 data with *I* > 2.0σ(*I*).

The X-ray crystal structures of (C₅Me₅)₃Pr, **3**, [(C₅Me₅)₂La]₂(μ-η²:η²-Se₂), **6**, [(C₅Me₅)₂La(THF)]₂(μ-η²:η²-Se₂), **7**, [(C₅Me₅)₂La]₂(μ-η³:η³-C₁₂N₂H₈), **8**, (C₅Me₅)₂Sm(O₂CC₅Me₅), **9**, and [(C₅Me₅)₂Sm(μ-I)]₃, **10**, were determined similarly. Experimental data are in Table 1 and in the Supporting Information.

(56) Evans, W. J.; Drummond, D. K.; Grate, J. W.; Zhang, H.; Atwood, J. L. *J. Am. Chem. Soc.* **1987**, *109*, 3928.

(57) SMART Software Users Guide, Version 5.1; Bruker Analytical X-Ray Systems, Inc.: Madison, WI, 1999.

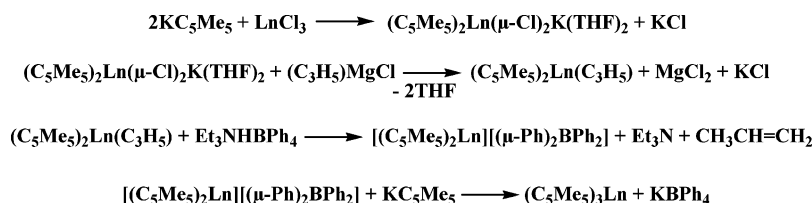
(58) SAINT Software Users Guide, Version 6.0; Bruker Analytical X-Ray Systems, Inc.: Madison, WI, 1999.

(59) Sheldrick, G. M. SADABS Version 2.05; Bruker Analytical X-Ray Systems, Inc.: Madison, WI, 2001.

(60) Sheldrick, G. M. SHELXTL Version 6.12; Bruker Analytical X-Ray Systems, Inc.: Madison, WI, 2001.

(61) International Tables for X-Ray Crystallography; Kluwer Academic Publishers: Dordrecht, 1992; Vol. C.

Scheme 1



Results

Synthesis of New $(\text{C}_5\text{Me}_5)_3\text{Ln}$ Complexes. Attempts to prepare $(\text{C}_5\text{Me}_5)_3\text{Ce}$ and $(\text{C}_5\text{Me}_5)_3\text{Pr}$ using the synthetic route that provided $(\text{C}_5\text{Me}_5)_3\text{Nd}$ and $(\text{C}_5\text{Me}_5)_3\text{Sm}$ in 90% yield,³³ Scheme 1, were unsuccessful. Although the immediate precursor to the $(\text{C}_5\text{Me}_5)_3\text{-Ln}$ complexes, i.e., $[(\text{C}_5\text{Me}_5)_2\text{Ln}][(\mu\text{-Ph})_2\text{BPh}_2]$, could be isolated in pure form for Ln = La–Pr, the reaction of these cations with KC_5Me_5 frequently gave the oxides, $[(\text{C}_5\text{Me}_5)_2\text{Ln}]_2(\mu\text{-O})$,^{41–44} which were crystallographically characterized in the case of La, Ce, and Pr.

In efforts to reduce oxide formation, the reactions of $[(\text{C}_5\text{Me}_5)_2\text{Ln}][(\mu\text{-Ph})_2\text{BPh}_2]$ with KC_5Me_5 were carried out in silylated glassware. In this way $(\text{C}_5\text{Me}_5)_3\text{Ln}$ complexes of the larger metals (Ln = La, **1**; Ce, **2**; Pr, **3**) could be prepared in high yield. Each complex exhibited the expected single resonance in its ^1H NMR spectrum: 1.997 for $(\text{C}_5\text{Me}_5)_3\text{La}$, 3.2 ppm for $(\text{C}_5\text{Me}_5)_3\text{Ce}$ ($\Delta\nu_{1/2} = 50$ Hz), and 6.8 ppm for $(\text{C}_5\text{Me}_5)_3\text{Pr}$ ($\Delta\nu_{1/2} = 5$ Hz). Since each of the $[(\text{C}_5\text{Me}_5)_2\text{Ln}]_2(\mu\text{-O})$ oxide alternative products^{41–44} also had single NMR resonances (La, 2.03; Ce, 1.93; Pr, 2.94 ppm), it was essential to identify the products by X-ray crystallography, Figure 2.

Structures of $(\text{C}_5\text{Me}_5)_3\text{Ce}$, **2, and $(\text{C}_5\text{Me}_5)_3\text{Pr}$, **3**.** Like $(\text{C}_5\text{Me}_5)_3\text{La}$, **1**,³⁴ $(\text{C}_5\text{Me}_5)_3\text{Nd}$, **4**,³³ and $(\text{C}_5\text{Me}_5)_3\text{Sm}$, **5**,¹ complexes **2** and **3** crystallize in space group $P6_3/m$. As is characteristic of these $(\text{C}_5\text{Me}_5)_3\text{Ln}$ structures, the three $(\text{C}_5\text{Me}_5)^-$ rings are equivalent and there are only three crystallographically independent Ln–C(C_5Me_5) distances. As shown in Table 2, these span a wide range. Both **2** and **3** have longer Ln–C(C_5Me_5) distances than any other trivalent cerium and praseodymium $(\text{C}_5\text{Me}_5)_2\text{Ln}$ -containing complexes in the literature, although there is only one praseodymium complex in the literature.^{4,62} The 2.850(2)–2.954(2) Å Ce–C(C_5Me_5) distances and 2.619 Å Ce–(ring centroid) length of $(\text{C}_5\text{Me}_5)_3\text{Ce}$ can be compared to the 2.74(3)–2.83(5) Å

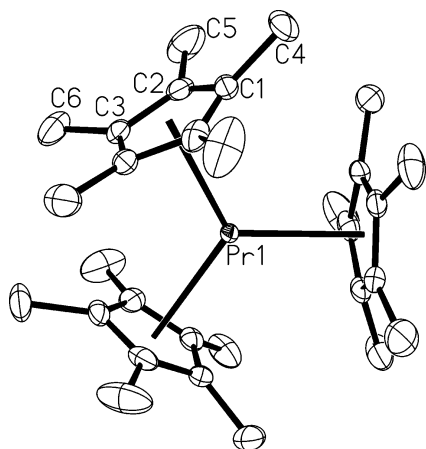


Figure 2. Thermal ellipsoid plot of $(\text{C}_5\text{Me}_5)_3\text{Pr}$, **3**, drawn at the 50% probability level.

Ce–C(C_5Me_5) average distances and 2.46–2.56 Å Ce–(ring centroid) distances for trivalent $(\text{C}_5\text{Me}_5)_2\text{Ce}$ -containing structures in the Cambridge Crystallographic Data Base.^{47,63–70}

The (C_5Me_5) ring centroid–Ln–(C_5Me_5 ring centroid) angles in **1–5** are rigorously 120° such that the ring centroids define a trigonal planar coordination environment around the metals. In comparison, the $(\text{C}_5\text{Me}_5)_2\text{Ce}$ -containing complexes mentioned above have analogous angles of 131.7 – 137.5° .

Table 2 shows that the bond lengths in **1–5** follow their ionic radii;²⁷ that is, the distances get longer as the metal size increases. This is typical for lanthanide complexes. However, for the sterically crowded $(\text{C}_5\text{Me}_5)_3\text{-Ln}$ complexes, a deviation could occur as the metal gets smaller and the crowding prevents the three $(\text{C}_5\text{Me}_5)^-$ ligands from getting any closer. Since the range of Ln–C(C_5Me_5) distances is so large, the error limits on the average Ln–C(C_5Me_5) bond distances are comparable to the difference in the ionic radii of one lanthanide to another. Hence, comparisons are made in Table 2 based on Ln–(ring centroid) distance and the longest Ln–C(C_5Me_5) distance in each compound. When the metals' radii are subtracted from the Ln–(ring centroid) distances,³ the result is 1.42 Å in each case; that is, the distances scale with the size of the metal. A similar result occurs when the radial sizes are subtracted from the longest Ln–C distance. In this case the difference is 1.76–1.78 Å.

The distances between the ring centroids in **1–5** decrease regularly with decreasing metal size: 4.577, 4.536, 4.500, 4.472, and 4.425 Å, respectively. Hence, in this series it is not evident that the closest packing of the three $(\text{C}_5\text{Me}_5)^-$ rings has been achieved. If this were the case, it might be that at some metal size the (C_5Me_5) ring centroid...(C_5Me_5 ring centroid) distance might have some minimum value that would not decrease even if the metal size decreased.

Another metrical parameter compared in the structures of **1–5** was the displacement of the methyl carbon atoms from the $(\text{C}_5\text{Me}_5)^-$ ring plane. Lanthanide com-

(62) Schumann, H.; Albrecht, I.; Loebel, J.; Hahn, E.; Hossain, M. B.; van der Helm, D. *Organometallics* **1986**, *5*, 1296.

(63) Hazin, P. N.; Huffman, J. C.; Bruno, J. W. *Organometallics* **1987**, *6*, 23.

(64) Rausch, M. D.; Moriarty, K. J.; Atwood, J. L.; Weeks, J. A.; Hunter, W. E.; Brittain, H. G. *Organometallics* **1986**, *5*, 1281.

(65) Hazin, P. N.; Lakshminarayan, C.; Brinen, L. S.; Knee, J. L.; Bruno, J. W.; Streib, W. E.; Folting, K. *Inorg. Chem.* **1988**, *27*, 1393.

(66) Booi, M.; Meetsma, A.; Teuben, J. H. *Organometallics* **1991**, *10*, 3246.

(67) Heeres, H. J.; Nijhoff, J.; Teuben, J. H.; Rogers, R. D. *Organometallics* **1993**, *12*, 2609.

(68) Deelman, B. J.; Booi, M.; Meetsma, A.; Teuben, J. H.; Kooijman, H.; Spek, A. L. *Organometallics* **1995**, *14*, 2306.

(69) Heeres, H. J.; Meetsma, A.; Teuben, J. H. *J. Organomet. Chem.* **1991**, *414*, 351.

(70) Heeres, H. J.; Maters, M.; Teuben, J. H.; Helgesson, G.; Jagner, S. *Organometallics* **1992**, *11*, 350.

Table 2. Comparative X-ray Data for (C₅Me₅)₃Ln Complexes

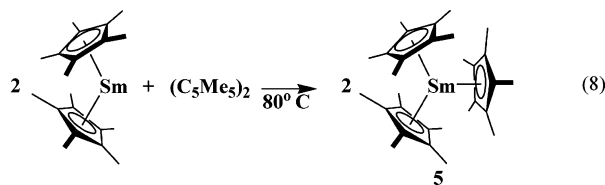
(C ₅ Me ₅) ₃ Ln	metal–centroid	centroid–centroid	Ln–C(C ₅ Me ₅)				effective 9-coordinate ionic radii	high Ln–C(C ₅ Me ₅) minus ionic radius	metal centroid minus ionic radius
			high	intermediate	low	mean			
(C ₅ Me ₅) ₃ Sm, 5	2.555	4.425	2.910(3)	2.817(2)	2.782(2)	2.82(5)	1.132	1.778	1.423
(C ₅ Me ₅) ₃ Nd, 4	2.582	4.472	2.927(2)	2.8421(14)	2.8146(13)	2.86(6)	1.163	1.764	1.419
(C ₅ Me ₅) ₃ Pr, 3	2.598	4.500	2.938(3)	2.856(2)	2.830(2)	2.86(4)	1.179	1.759	1.419
(C ₅ Me ₅) ₃ Ce, 2	2.619	4.536	2.954(2)	2.8760(16)	2.8497(16)	2.88(4)	1.196	1.758	1.423
(C ₅ Me ₅) ₃ La, 1	2.642	4.577	2.975(3)	2.896(2)	2.8732(19)	2.91(5)	1.216	1.759	1.426

Table 3. Displacement of the Methyl Carbon Atoms from the (C₅Me₅)[−] Ring Plane (Å)

	(C ₅ Me ₅) ₃ Ln				
	(C ₅ Me ₅) ₃ La 1	(C ₅ Me ₅) ₃ Ce 2	(C ₅ Me ₅) ₃ Pr 3	(C ₅ Me ₅) ₃ Nd 4	(C ₅ Me ₅) ₃ Sm 5
displacement of C(4) from ring plane	0.501	0.503	0.517	0.519	0.521
displacement of C(6) from ring plane	0.309	0.324	0.332	0.341	0.362
displacement of C(5) from ring plane	0.160	0.169	0.168	0.173	0.175

plexes with normal Ln–C(C₅Me₅) distances have out-of-plane displacements of 0.09–0.31 Å.³⁴ As shown in Table 3, the displacements for the three crystallographically independent methyl carbons in **1–5** span a range of 0.160–0.521 Å. In general the displacements increase regularly as the metal size decreases. This is consistent with increasing steric crowding and decreasing (C₅Me₅ ring centroid)⋯(C₅Me₅ ring centroid) distance. However, it should be noted that the differences between complexes are small and the magnitude of the out-of-plane displacement does not correlate in a regular way with the Ln–C bond distances. The methyl with the largest displacement is attached to the ring carbon with the longest Ln–C bond in each complex, but the smallest Ln–C bond in each case does not have a methyl with the smallest displacement. Only the methyl displacement for the longest Ln–C bond is outside the range found in other (C₅Me₅)[−] lanthanide complexes.³⁴ This carbon is the one located in the trigonal plane of the complex, C4.

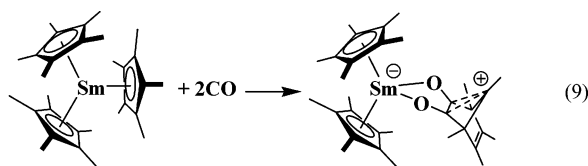
New Synthesis of (C₅Me₅)₃Sm. Although it was originally assumed that (C₅Me₅)₃Sm was too sterically crowded to exist,¹ once the first synthesis was discovered, eq 1, three additional syntheses were subsequently identified, eqs 5–7. In the course of investigating the reductive reactivity of (C₅Me₅)₃Sm as described below, the relationship of (C₅Me₅)₃Sm to (C₅Me₅)₂Sm and (C₅Me₅)₂ was of interest. Although no reaction was observed between the latter two species in 12 h at 25 °C, (C₅Me₅)₂Sm reacts with (C₅Me₅)₂ in 2 h at 80 °C in benzene to form (C₅Me₅)₃Sm in 84% yield as shown in eq 8. This provided a fifth synthesis of (C₅Me₅)₃Sm.



Comparative Reactivity of 1–5. The reaction chemistry of **1–4** was compared with that of **5** to see how reactivity changed with the size of the metal and the concomitant change in steric crowding.

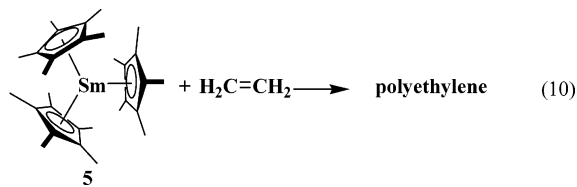
Alkyl-like Reactivity. Carbon Monoxide. The reactivity of **1–4** with CO was examined to see if nonclassical carbonium ion complexes of the type (C₅Me₅)₂Ln(O₂C₇Me₅) found for Sm,⁶ eq 9, and Nd¹³

could be obtained with the larger metals. (C₅Me₅)₃Pr



and (C₅Me₅)₃Ce react with CO at 1 atm in a manner analogous to (C₅Me₅)₃Sm and (C₅Me₅)₃Nd to produce compounds with spectral characteristics similar to those of the previously identified (C₅Me₅)₂Ln(O₂C₇Me₅) complexes. The IR spectra of the Ce and Pr compounds are almost identical to those of the Nd and Sm analogues. The pattern of resonances in the ¹H NMR spectra also matches those for Nd and Sm: two resonances of intensity 15 (Ce, 2.17, 2.43; Pr, 5.4, 6.1 ppm) and three resonances with a 3:6:6 intensity ratio (Ce, 5.59, 2.34, −0.55; Pr, 2.7, 1.0, −12.7 ppm) as expected. (C₅Me₅)₃La did not react with CO under comparable conditions. Only after several days at 50 °C did the (C₅Me₅)₃La/CO reaction give a new pattern of resonances in the ¹H NMR spectrum consistent with the formation of a (C₅Me₅)₂La(O₂C₇Me₅) product. Hence, eq 9 applies at room temperature only to Ce, Pr, Nd, and Sm.

Ethylene. (C₅Me₅)₃Sm readily polymerizes ethylene to a high molecular weight polymer, eq 10.⁷ (C₅Me₅)₃Nd

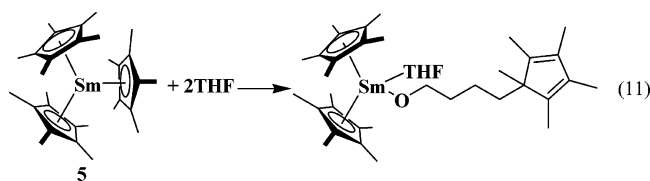


reacts similarly. Unfortunately, the polyethylene formed in these reactions is too high in molecular weight to be studied by NMR or field desorption mass spectroscopy (FDMS).⁷¹ (C₅Me₅)₃Ce and (C₅Me₅)₃Pr polymerize ethylene under similar reaction conditions, but were considerably less active. No polymerization reactivity is observed for (C₅Me₅)₃La. Hence, eq 10 applies to Ce, Pr, Nd, and Sm.

Tetrahydrofuran. (C₅Me₅)₃Sm readily reacts with any available THF to form the ring-opened product

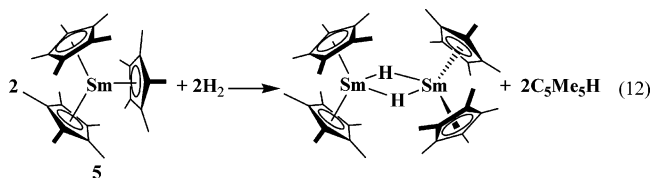
(71) Evans, W. J.; DeCoster, D. M.; Greaves, J. *Macromolecules* **1995**, *28*, 7929.

$(C_5Me_5)_2Sm[O(CH_2)_4C_5Me_5](THF)$, eq 11.^{8,72,73} $(C_5Me_5)_3Nd$

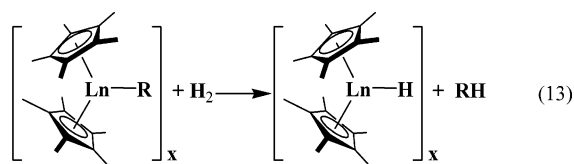


reacts instantaneously with several equivalents of THF, but appears to form a mixture of products. Although the paramagnetism of Nd(III) does not permit detailed analysis, the 1H NMR spectrum contains several sets of peaks that could be interpreted as the ring-opened product, $(C_5Me_5)_2Nd[O(CH_2)_4C_5Me_5](THF)$. $(C_5Me_5)_3Pr$ is not completely decomposed by 2 equiv of THF, but it is completely consumed when dissolved in neat THF. $(C_5Me_5)_3Ce$ also reacts with THF and, like the Nd and Pr analogues, the NMR spectra are not definitive. With $(C_5Me_5)_3La$ no reaction was observed with 1–10 equiv of THF, even at elevated temperatures. However, when $(C_5Me_5)_3La$ is dissolved in neat THF at room temperature, the 1H NMR spectroscopy is consistent with the ring-opened product.⁷³ Hence, eq 11 applies to all the lanthanides in this study.

Hydrogen. $(C_5Me_5)_3Sm$ readily reacts with H_2 to form the hydride complex $[(C_5Me_5)_2Sm(\mu-H)]_2$,⁷⁴ eq 12.⁷



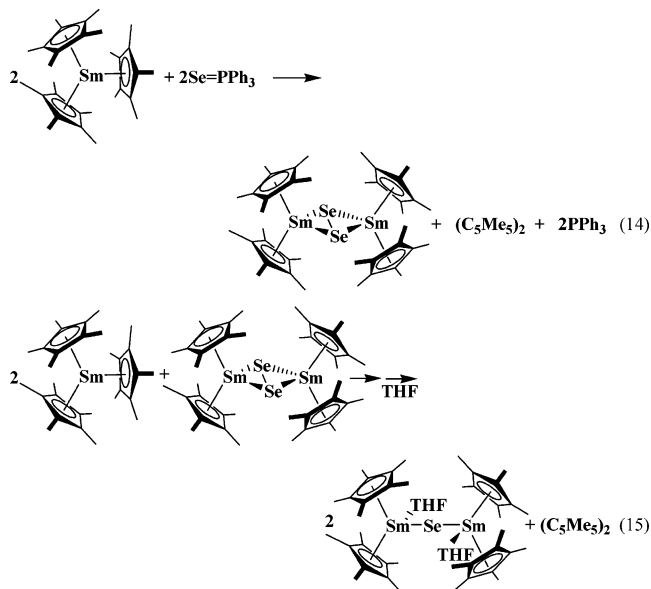
Formation of lanthanide hydrides by hydrogenolysis is a characteristic reaction of lanthanide alkyls, eq 13.^{49,50,74–77} $(C_5Me_5)_3Nd$ reacts similarly with H_2 to form



the corresponding $[(C_5Me_5)_2NdH]_x$,^{49,50} but $(C_5Me_5)_3Pr$ requires 40 psi of H_2 to make $[(C_5Me_5)_2PrH]_x$ and C_5Me_5H . $(C_5Me_5)_3La$ does not react in this manner, and even at elevated pressures there was no NMR evidence for the formation of C_5Me_5H and the lanthanide hydride complex.⁴⁹ Hence, eq 12 applies to only Ce, Pr, Nd, and Sm.

Comparative Sterically Induced Reductive Reactivity of 1–5. Triphenylphosphine Selenide. Trivalent $(C_5Me_5)_3Sm$, **5**, has been found to exhibit reductive reactivity with a variety of substrates. Of

these, the substrate that has allowed the most direct comparison across the series is $Se=PPh_3$. As reported earlier, **5** reduces $Se=PPh_3$ stepwise to a perselenide $(Se_2)^{2-}$ product, $[(C_5Me_5)_2Sm]_2(\mu-\eta^2: \eta^2-Se_2)$, eq 14, and then to a $(Se)^{2-}$ selenide, $[(C_5Me_5)_2Sm(THF)]_2(\mu-Se)$, eq 15.¹⁰ The less sterically crowded $(C_5Me_5)_3Nd$, **4**, can accomplish only the first reduction under comparable conditions, i.e., eq 14.¹⁰



The least sterically crowded complex of the 1–5 series, $(C_5Me_5)_3La$, is also capable of reducing $Se=PPh_3$, eq 14. $(C_5Me_5)_3La$ reacts with $Ph_3P=Se$ in toluene to form a red product with a 1H NMR resonance at 2.17 ppm in C_6D_6 . Also observed were PPh_3 and $(C_5Me_5)_2$, the characteristic byproduct of sterically induced reduction. An X-ray diffraction study verified that the product was the perselenide complex $[(C_5Me_5)_2La]_2(\mu-\eta^2: \eta^2-Se_2)$, **6**, Figure 3, eq 14. Like the Nd system, the use of more than 1 equiv of $(C_5Me_5)_3La$ per $Se=PPh_3$ does not lead to further reduction, eq 15. Hence, eq 14 is viable for even the least crowded $(C_5Me_5)_3Ln$, $Ln = La$, but eq 15 applies to only Sm.

Addition of THF to $[(C_5Me_5)_2La]_2(\mu-\eta^2: \eta^2-Se_2)$, **6**, and recrystallization also gave X-ray quality crystals, and these were identified as the THF adduct, $[(C_5Me_5)_2La(THF)]_2(\mu-\eta^2: \eta^2-Se_2)$, **7**, Figure 4. This provides a rather unusual case in which both the n -coordinate and $(n+1)$ -coordinate complex can be crystallographically characterized with the same ligand set.⁷⁷ Since La is

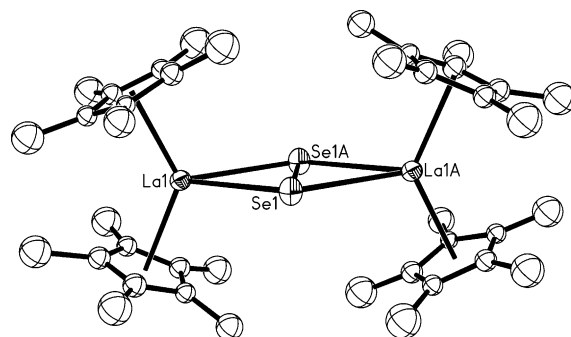


Figure 3. Thermal ellipsoid plot of $[(C_5Me_5)_2La]_2(\mu-\eta^2: \eta^2-Se_2)$, **6**, drawn at the 50% probability level.

(72) Evans, W. J.; Ulibarri, T. A.; Chamberlain, L. R.; Ziller, J. W.; Alvarez, D., Jr. *Organometallics* **1990**, *9*, 2124.

(73) Schumann, H.; Glanz, M.; Hemling, H.; Görlitz, F. H. *J. Organomet. Chem.* **1993**, *462*, 155.

(74) Evans, W. J.; Bloom, I.; Hunter, W. E.; Atwood, J. L. *J. Am. Chem. Soc.* **1983**, *105*, 1401.

(75) Evans, W. J.; Meadows, J. H.; Wayda, A. L.; Hunter, W. E.; Atwood, J. L. *J. Am. Chem. Soc.* **1982**, *104*, 2008.

(76) Evans, W. J.; Meadows, J. H.; Hunter, W. E.; Atwood, J. L. *J. Am. Chem. Soc.* **1984**, *106*, 1291.

(77) Evans, W. J.; Drummond, D. K.; Hughes, H.; Zhang, H.; Atwood, J. L. *Polyhedron* **1988**, *7*, 1693.

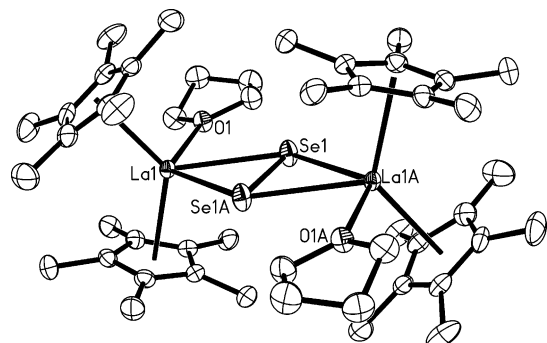
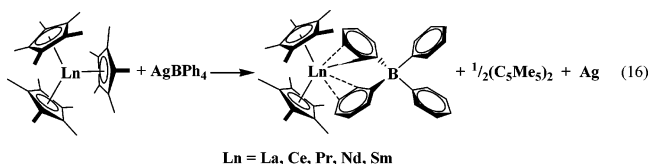


Figure 4. Thermal ellipsoid plot of [(C₅Me₅)₂La(THF)]₂-(μ-η²:η²-Se₂), **7**, drawn at the 50% probability level.

larger than Nd and Sm, it is reasonable that a THF adduct could form. Evidently, in this case, the slightly larger metal allowed crystallization of a THF adduct, whereas the Nd and Sm systems have yielded only unsolvated (Se₂)²⁻ complexes suitable for X-ray crystallography.

Structures of [(C₅Me₅)₂La]₂(μ-η²:η²-Se₂), **6, and [(C₅Me₅)₂La(THF)]₂(μ-η²:η²-Se₂), **7**.** Crystals of **6** are isomorphous with the Nd and Sm analogues previously described.¹⁰ The metrical parameters for the metallocene part of the complex are normal. The 2.394(2) Å Se(1)–Se(1A) distance is in the Se–Se single bond range and is similar to the 2.389(2) and 2.396(2) Å distances in the Nd and Sm analogues, respectively. The structure of **7**, the THF solvate of **6**, is similar, but the metrical parameters in the metallocene part of the complex are different due to the higher coordination number and the reduced Lewis acidity of the solvated metal center.²⁷ Hence, the La–(C₅Me₅) ring centroid distances are 2.583 and 2.594 Å in **7** compared to 2.506 and 2.529 Å in **6**. The (C₅Me₅ ring centroid)–La–(C₅Me₅ ring centroid) angle in **7** is 129.7° compared to 131.7° in **6**. The 3.1143(4) and 3.1377(4) Å La–Se distances in **7** are also longer than the 3.068(1) and 3.070(1) Å analogues in **6**. The 2.3694(7) Å Se–Se distance is similar to that in **6**.

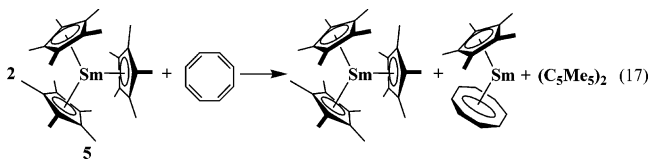
AgBPh₄. All of the complexes, **1–5**, react with AgBPh₄ to form [(C₅Me₅)₂Ln][(μ-Ph)₂BPh₂],³³ Ag, and (C₅Me₅)₂, eq 16. This reaction was easily verified since



all of the [(C₅Me₅)₂Ln][(μ-Ph)₂BPh₂] products were previously characterized. This reaction was examined to see if the (C₅Me₅)₃Ln complexes would reduce Ag¹⁺ to Ag and establish a minimum capacity to effect a reduction of about –0.3 V vs SCE. However, since sterically crowded complexes that contain actinide metal centers have been observed to undergo ionic metathesis reactions to displace (C₅Me₅)⁻ ligands,¹⁶ the reaction could also occur via ionic metathesis between (BPh₄)⁻ and (C₅Me₅)⁻. This would form [(C₅Me₅)₂Ln][(μ-Ph)₂BPh₂] and (C₅Me₅)Ag, which could decompose homolytically to (C₅Me₅)₂ and Ag on the basis of related Cu^{50,78,79} and

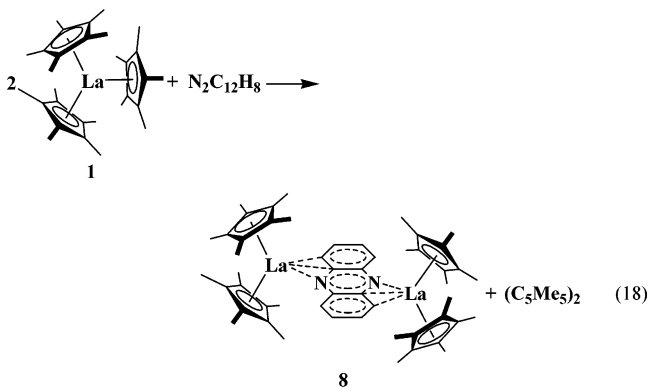
Hg²³ chemistry. (C₅Me₅)₃Sm does not react with NaBPh₄, however.

1,3,5,7-Cyclooctatetraene. In contrast to the reactions with Se=PPh₃ and AgBPh₄, in which all examples of the (C₅Me₅)₃Ln series display some reactivity, only the most crowded Sm complex **5** reduces C₈H₈. Hence, like divalent (C₅Me₅)₂Sm,¹ eq 1, trivalent (C₅Me₅)₃Sm reduces C₈H₈ to (C₈H₈)²⁻ and forms (C₅Me₅)Sm(C₈H₈), eq 17.⁸



In contrast, **1–4** are not powerful enough reductants to reduce C₈H₈. Since C₈H₈ has a first reduction potential of –1.83 V (vs SCE) and a second of –1.99 V, this defines a limit on the reductive capacity of **1–4**.

Phenazine. To better estimate the reduction potential of the least sterically crowded complex, (C₅Me₅)₃La, **1**, was treated with a variety of polycyclic aromatic substrates with well-established redox potentials that had been used to characterize the reduction capacity of (C₅Me₅)₂Sm.^{50,80} Since complex **1** is not as reducing as (C₅Me₅)₂Sm, it does not reduce most of these including benzanthracene, which has first and second reduction potentials of –1.58 and –1.93 V vs SCE.⁸¹ However, **1** does reduce phenazine, which has a reduction potential of –0.364 V vs SCE, eq 18.⁸² The reaction of (C₅Me₅)₃La



with phenazine in a 2:1 ratio causes an instant color change from yellow to dark red. After 24 h, ¹H NMR spectroscopy indicated that consumption of the starting materials with concomitant formation of [(C₅Me₅)₂La]₂(μ-η³:η³-C₁₂N₂H₈), **8**, and (C₅Me₅)₂ had occurred. (C₅Me₅)₃Sm reacts similarly.

X-ray crystallography confirmed the existence of **8**, Figure 5, eq 18. This structure is similar to those of [(C₅Me₅)₂Sm]₂(μ-η³:η³-C₁₂N₂H₈)(toluene), made from (C₅Me₅)₂Sm and phenazine,⁵¹ and [(C₅Me₅)₂La]₂(μ-η³:η³-C₁₂N₂H₈)(Et₂O), made from (C₅Me₅)₂LaCl₂K(DME)₂ and Na₂(C₁₂N₂H₈).⁵² Although all three structures crystallized in *P* $\bar{1}$ with similar cell constants, they are not isomorphous since each crystallized with a different

(80) Fedushkin, I. L.; Bochkarev, M. N.; Dechert, S.; Schumann, H. *Chem. Eur. J.* **2001**, *7*, 3558.

(81) De Boer, E. *Adv. Organomet. Chem.* **1964**, *2*, 115.

(82) Nechaeva, O. N.; Pushkareva, Z. V. *Zh. Obshch. Khim.* **1958**, *28*, 2693.

(78) Zybilla, C.; Müller, G. *Organometallics* **1987**, *6*, 2489.

(79) Lettko, L.; Rausch, M. D. *Organometallics* **2000**, *19*, 4060.

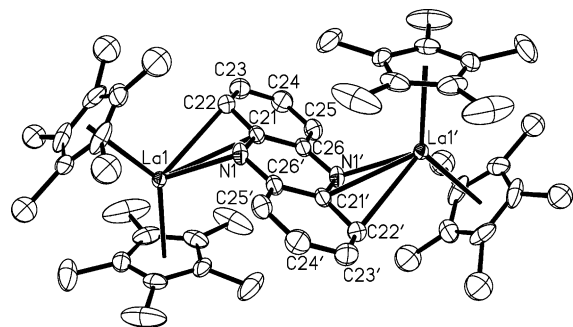


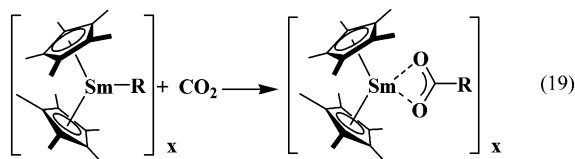
Figure 5. Thermal ellipsoid plot of $[(C_5Me_5)_2La]_2(\mu-\eta^3:\eta^3-C_{12}N_2H_8)$, **8**, drawn at the 50% probability level.

solvent molecule. In this case, **8** crystallized with benzene in the unit cell. The structure is very similar to those described in the literature with the phenazine dianion planar to within 0.025 Å and the main interaction with the metal being the 2.447(2) Å La(1)–N(1) distance. The C(21) and C(22) La–C distances are 2.910(2) and 2.929(3) Å, respectively. The C–C and C–N distances in the phenazine dianion were all between 1.374(4) and 1.406(4) Å.

As expected, $(C_5Me_5)_3Sm$ also reduces phenazine to make the previously characterized samarium analogue of **8**, $[(C_5Me_5)_2Sm]_2(\mu-\eta^3:\eta^3-C_{12}N_2H_8)$, originally made from $(C_5Me_5)_2Sm$.⁵¹

New Reactions of $(C_5Me_5)_3Ln$ Complexes. Several new reactions of $(C_5Me_5)_3Sm$ are reported below. These reactions were done with samarium since it was the first $(C_5Me_5)_3Ln$ complex available and also because in many cases the reactions generate known $[(C_5Me_5)_2SmX]_n$ products (X = anion). Due to the broad reactivity of $(C_5Me_5)_2Sm$, more $[(C_5Me_5)_2LnX]_n$ compounds are in the literature for samarium than for other lanthanides.^{4,83}

Carbon Dioxide. CO_2 is an interesting substrate for $(C_5Me_5)_3M$ complexes since it could react by either of the pathways identified so far for these complexes, eq 2 or eq 3. One of the characteristic reactions of alkyl complexes of electropositive metals is the insertion of CO_2 to make carboxylates, eq 19. This reaction has been



examined with a variety of trivalent samarium metallocene complexes including $(C_5Me_5)_2Sm(C_3H_5)$,⁸¹ $[(C_5Me_5)_2SmPh]_2$,⁸⁴ and $(C_5Me_5)_2Sm(CH_2Ph)$.⁸⁵ Jutzi has previously reported that C_5Me_5Li reacts with CO_2 to make an intermediate, presumably $C_5Me_5CO_2Li$, that reacts with Me_3SiCl to form $C_5Me_5CO_2SiMe_3$.⁸⁶ Alternatively, CO_2 can be reduced by the divalent lanthanide

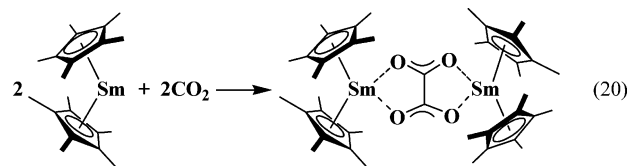
(83) For example, the Cambridge Crystallographic Database lists 183 structurally characterized complexes containing a $(C_5Me_5)_2Sm$ unit vs 141 structures containing $(C_5Me_5)_2Ln$ units in which Ln = all the rest of the lanthanide elements.

(84) Evans, W. J.; Seibel, C. A.; Ziller, J. W.; Doedens, R. J. *Organometallics* **1998**, *17*, 2103.

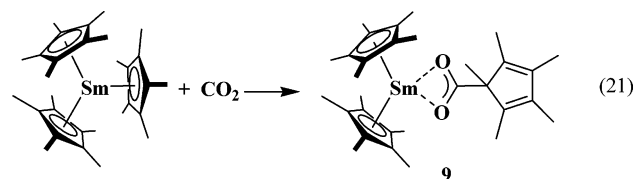
(85) Evans, W. J.; Perotti, J. M.; Ziller, J. W. *J. Am. Chem. Soc.* **2005**, *127*, 3894.

(86) Jutzi, P.; Kohl, F. X. *Chem. Ber.* **1987**, *120*, 1539.

metallocene $(C_5Me_5)_2Sm$ to form an oxalate dianion, $(C_2O_4)^{2-}$, eq 20.⁸⁷



The reaction of CO_2 with $(C_5Me_5)_3Sm$ proceeds with insertion into a Sm– C_5Me_5 unit to form a carboxylate with a pentamethylcyclopentadiene group as a substituent, $(C_5Me_5)_2Sm(O_2CC_5Me_5)$, **9**, eq 21. The structure of



9 was confirmed by X-ray crystallography, Figure 6. To our knowledge this is the first X-ray structure of a carboxylate containing pentamethylcyclopentadiene as a substituent. The reaction between $(C_5Me_5)_3Sm$ and CO_2 occurs quickly as a frozen solution of $(C_5Me_5)_3Sm$ is warmed to room temperature under CO_2 . The 1H NMR spectrum of **9** contains a 2:2:1 pattern of methyl groups consistent with a pentamethylcyclopentadiene substituent as well as a resonance of relative intensity 10 for the pentamethylcyclopentadienide methyl groups. Since both the 1H and ^{13}C NMR spectra show one type of $(C_5Me_5)^-$ environment, in solution **9** does not maintain the structure found in the solid state. 1H NMR and IR spectroscopy indicate that $(C_5Me_5)_3Nd$ reacts analogously with CO_2 .

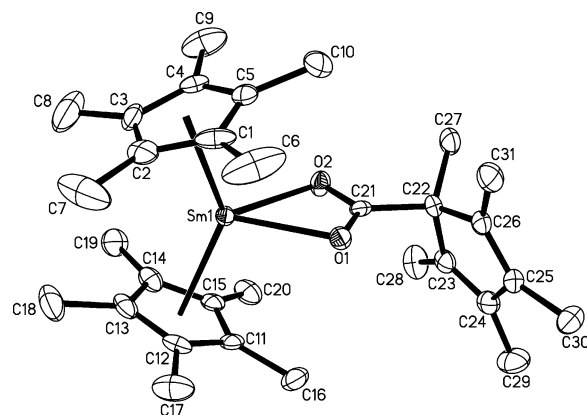
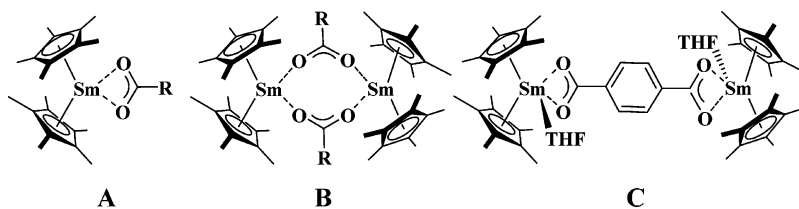


Figure 6. Thermal ellipsoid plot of $(C_5Me_5)_2Sm(O_2CC_5Me_5)$, **9**, drawn at the 50% probability level.

Structure of $(C_5Me_5)_2Sm(O_2CC_5Me_5)$, **9.** The structure of **9**, Figure 6, has metrical parameters for the $[(C_5Me_5)_2Sm]^+$ component typical of eight-coordinate trivalent decamethylsamarocene complexes⁴ with a 138.7° (C_5Me_5 ring centroid)–Sm–(C_5Me_5 ring centroid) angle, 2.409–2.425 Å ring centroid distances, and a 2.69(3) Å Sm–C(C_5Me_5) average distance. The structure is atypical of carboxylates of lanthanide metallocenes in that it is an unsolvated monomer, A, Scheme

(87) Evans, W. J.; Seibel, C. A.; Ziller, J. W. *Inorg. Chem.* **1998**, *37*, 770, and references therein.

Scheme 2



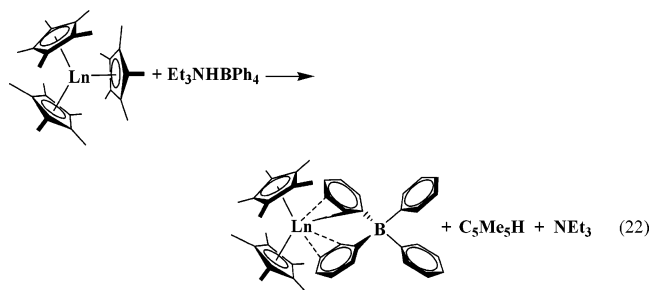
2. The [(C₅Me₅)₂Sm(μ-η²-O₂CR)]₂ complexes (R = CH₂CH=CH₂,⁸⁴ CH₂Ph,⁸⁵ C₆H₄Me-*m*,⁸⁵ and Ph⁸⁴) have bridging carboxylates which generate eight-atom

SmOCOSmOCO rings, B, Scheme 2. The terephthalic acid derivative (C₅Me₅)₂Sm(THF)(μ-η²: η²-O₂CC₆H₄-CO₂)Sm(THF)(C₅Me₅)₂⁸⁴ is more similar to **9** in that

four-membered SmOCO rings are formed by a single carboxylate attached to each metal, but it differs in that it is solvated, C, Scheme 2. The unsolvated monomeric CS₂ insertion product (C₅Me₅)₂Sm(S₂CCH₂CH=CH₂)⁸⁴ is probably closest structurally to (C₅Me₅)₂Sm(O₂CC₅-Me₅).

The 2.388(3) and 2.409(3) Å Sm–O(1) and Sm–O(2) lengths and identical 1.271(5) and 1.271(6) Å O(1)–C(11) and O(2)–C(11) distances show complete delocalization in the carboxylate. The 1.527(6) Å C(21)–C(22) distance is normal for a single bond. The 54.78(11)° O(1)–Sm–O(2) angle is much smaller than the 87.4(1)–90.8(1)° angles in the bimetallic [(C₅Me₅)₂Sm(μ-η²-O₂CR)]₂ complexes and is more similar to the 63.2(1)° angle in monometallic (C₅Me₅)₂Sm(S₂CCH₂CH=CH₂).

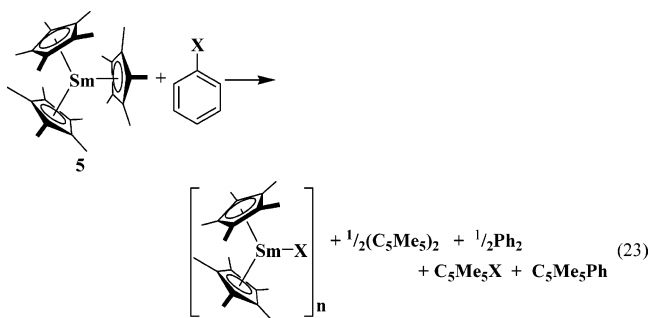
Et₃NHBPh₄. Et₃NHBPh₄ is another reagent that could react in two ways with the (C₅Me₅)₃Ln complexes. Reduction according to eq 3 would form [(C₅Me₅)₂Ln]–[(μ-Ph)₂BPh₂] along with H₂, NEt₃, and (C₅Me₅)₂ as byproducts.¹⁶ If the (C₅Me₅)₃Ln complexes react as pseudo-alkyl complexes, protonolysis would form only C₅Me₅H and NEt₃ as the byproducts. (C₅Me₅)₃Sm, (C₅Me₅)₃Nd, and (C₅Me₅)₃Pr all react cleanly with Et₃NHBPh₄ to yield [(C₅Me₅)₂Ln]–[(μ-Ph)₂BPh₂], C₅Me₅H, and NEt₃, eq 22.



Alkyl Halides. To examine further the one-electron reduction reactivity of (C₅Me₅)₃Ln complexes and the (C₅Me₅)[–]/C₅Me₅ redox couple of eq 3, reactions of (C₅Me₅)₃Sm with aryl halides and alkyl halide radical clock reagents⁸⁸ were examined. (C₅Me₅)₃Sm reacts rapidly with alkyl and aryl halides, but unfortunately a mixture of products is formed, which complicates the reaction pathway analysis.

(C₅Me₅)₃Sm reacts with 1–3 equiv of the aryl halides, C₆H₅X (X = F, Cl, Br, I), to make product mixtures that

include (C₅Me₅)₂, the byproduct expected from sterically induced reduction according to eq 3, as well as biphenyl, C₅Me₅(C₆H₅), and C₅Me₅X, eq 23. The major samarium



product of these reactions is [(C₅Me₅)₂SmX]_n. The [(C₅Me₅)₂Sm(μ-Cl)]₃ complex has been previously characterized by X-ray crystallography and found to be trimeric.⁵⁶ The analogous structure of [(C₅Me₅)₂Sm(μ-I)]₃, **10**, is reported here for the first time, Figure 7. The organosamarium product of the reaction with C₆H₅Br has limited solubility like the other analogues and is expected to be similar.⁸⁹ The degree of aggregation of the fluoride is unknown, but the ether solvate has previously been reported.⁹⁰ The ¹H NMR shifts in C₆D₆ of these four unsolvated samarocene halide products, [(C₅Me₅)₂SmX]_n, change in a periodic sequence: X = I, 0.66; Br,⁸⁹ 0.41; Cl, –0.22; F, –0.29 ppm.

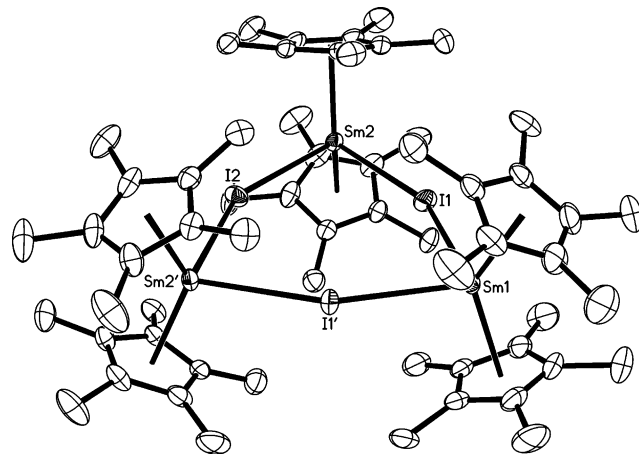


Figure 7. Thermal ellipsoid plot of [(C₅Me₅)₂Sm(μ-I)]₃, **10**, drawn at the 50% probability level.

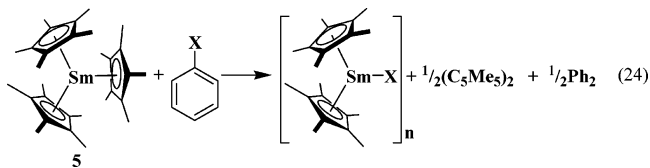
The relative reactivity of the C₆H₅X reagents with (C₅Me₅)₃Sm is I > Br > Cl > F, as expected. The iodide reacts upon mixing, the bromide is consumed in 8 h, the chloride still has unreacted (C₅Me₅)₃Sm after 24 h,

(89) Nolan, S. P.; Stern, D.; Marks, T. J. *J. Am. Chem. Soc.* **1989**, *111*, 7844.

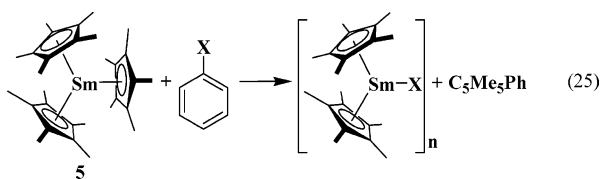
(90) Watson, P. L.; Tulip, T. H.; Williams, I. *Organometallics* **1990**, *9*, 1999.

(88) Griller, D.; Ingold, K. U. *Acc. Chem. Res.* **1980**, *13*, 317.

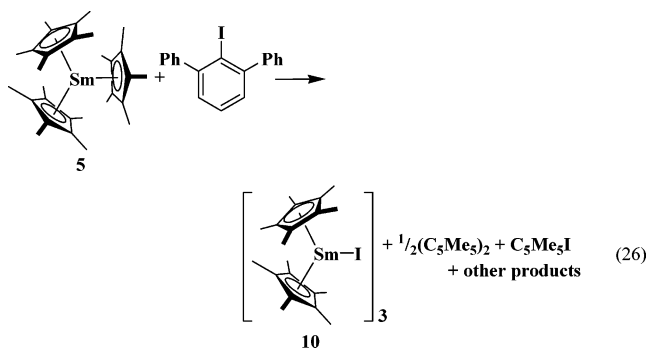
and the fluoride requires heating with excess C_6H_5F for 2 days. The presence of $(C_5Me_5)_2$ in the reaction mixtures suggests that one part of eq 23 involves sterically induced reduction reactivity according to eq 24. How-



ever, the presence of the $C_5Me_5(C_6H_5)$ and C_5Me_5X byproducts indicates that other reactions are also occurring. Nucleophilic substitution involving pentamethylcyclopentadienyl samarium moieties has previously been identified as a complicating reaction in earlier studies of reduction of aryl halides with divalent $(C_5Me_5)_2Sm$.^{53,54,91} Hence, reactions such as eq 25 may also occur as part of eq 23.

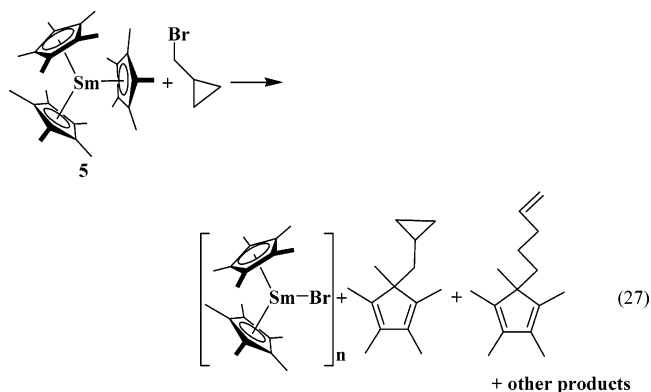


The reaction of $(C_5Me_5)_3Sm$ with terphenyl iodide was examined to see if reduction would occur even with this very sterically crowded halide. Although no reaction occurs upon mixing (in contrast to the immediate reaction of **5** and C_6H_5I above), 86% of the $(C_5Me_5)_3Sm$ is consumed over 3 days and the 1H NMR spectrum revealed the presence of $(C_5Me_5)_2$, C_5Me_5I , and $[(C_5Me_5)_2Sm(\mu-I)]_3$, eq 26.



Reactions of $(C_5Me_5)_3Sm$ with radical clocks⁸⁸ were also examined. $(C_5Me_5)_3Sm$ reacts with the bromomethylcyclopropane to produce a 3:1 mixture of (cyclopropyl)- and (allylcarbinyl)pentamethylcyclopentadienes, eq 27. The presence of the ring-opened product is consistent with radical reactivity, but the isolation of a mixture of products shows that other pathways could also occur. In comparison, KC_5Me_5 reacted with bromomethylcyclopropane to exclusively form $(\overline{CH_2CH_2CH})-CH_2C_5Me_5$ and KBr .

Some preliminary halide reactions were also conducted with $(C_5Me_5)_3Nd$. This less crowded complex reacts with 1 equiv of C_6H_5I to yield $[(C_5Me_5)_2Nd(\mu-I)]_3$,



which was determined by X-ray crystallography⁹² to have a structure like that of $[(C_5Me_5)_2Sm(\mu-I)]_3$. However, $(C_5Me_5)_3Nd$ does not appear to react with C_6H_5Br or C_6H_5Cl up to 60 °C. In fact, C_6H_5Cl can be used as a solvent for the preparation of $(C_5Me_5)_3Nd$ from $[(C_5Me_5)_2Nd][(\mu-Ph)_2BPh_2]$ and KC_5Me_5 . Hence, when solvents more polar than toluene are desirable for $(C_5Me_5)_3Ln$ reactions, C_6H_5Cl is an option.

Consistent with the above results, the less crowded $(C_5Me_5)_3Pr$ is even less reactive. It does not react with 1 equiv of C_6H_5I after 24 h at room temperature. Only upon heating is a reaction observed.

Structure of $[(C_5Me_5)_2Sm(\mu-I)]_3$, **10.** In the solid state, $(C_5Me_5)_2SmI$ crystallizes as a trimer, Figure 7, in a structure similar to its congener, $[(C_5Me_5)_2Sm(\mu-Cl)]_3$.⁵³ The two compounds are isomorphous and have planar $Sm_3(\mu-X)_3$ substructures (to within 0.0061 Å for the iodide). The 133.4° and 133.5° (C_5Me_5 ring centroid)–Sm–(C_5Me_5 ring centroid) angles, the 2.43 Å Sm–(C_5Me_5 ring centroid) distances, and the 2.71(2) Å Sm–C(C_5Me_5) average distance are normal for eight-coordinate metallocenes. The chloride analogue has similar 2.44–2.47 Å Sm–(C_5Me_5 ring centroid) distances, but the 127.8–128.2° (ring centroid)–Sm–(ring centroid) angles are much smaller, indicating more steric congestion with the smaller bridging halide. The three crystallographically independent Sm–($\mu-I$) lengths fall in a narrow range, 3.1607(3)–3.1886(2) Å, such that the complex approaches D_{3h} symmetry. The Sm–($\mu-I$) distances are approximately 0.30 Å longer than the analogous chloride distances in comparison to the 0.39 Å difference in the Shannon ionic radii of these halides.²⁷ The 150.42(2)° and 154.43(1)° Sm–($\mu-I$)–Sm angles are similar to the 154.0(3)° and 158.2(3)° values in the chloride analogue. The degree of staggering of the $(C_5Me_5)^-$ rings on each Sm leads to a range of torsional C–(C_5Me_5 ring centroid)–(C_5Me_5 ring centroid)–C angles of 21.5–27.8° in contrast to the 35–47° range in the chloride.

Discussion

Synthesis. Since the La, Ce, Pr, and Nd analogues of $(C_5Me_5)_3Sm$ should be less crowded due to the larger size of these metals, it was anticipated that these complexes should be stable enough to isolate if a

(92) $[(C_5Me_5)_2Nd(\mu-I)]_3$ crystallizes in the same group as $[(C_5Me_5)_2Sm(\mu-I)]_3$, but the unit cell and volume are different because two molecules of toluene per formula unit are present. The data were of sufficient quality to get connectivity, but not to discuss metrical parameters.

synthetic pathway was available. Surprisingly, the sterically less crowded La, Ce, and Pr complexes, **1–3**, required syntheses in silylated glassware, whereas the Nd and Sm compounds, **4** and **5**, did not. Hence, on the basis of the synthetic difficulty, it appeared that the complexes of the larger metals would be more reactive, giving a reactivity order of **1** > **2** > **3** > **4** > **5**. This is often the case in the chemistry of organolanthanides with conventional bond distances. The larger metals form complexes that are sterically less saturated, and the extra space in the coordination environment can make them more reactive by providing reaction pathways not available to the complexes of the smaller metals.^{2,24–26}

However, the order of reactivity of the (C₅Me₅)₃Ln complexes is actually **5** > **4** > **3** > **2** > **1**. The factor that appears to drive the reactivity of these long-bond organometallic complexes in the reactions examined in this study is the amount of steric crowding, not the amount of steric unsaturation. Hence, the larger metals do not provide extra reaction pathways via open coordination sites, but instead they relieve the steric crowding and thereby reduce the reactivity.

This suggests that the observed difficulty in preparing **1–3** vs **4** and **5** may be related to the relative stability of the precursors as opposed to the targeted (C₅Me₅)₃Ln complexes. Since the [(C₅Me₅)₂Ln]₂(μ-O) oxides^{41–44} are the common byproducts when the crucial conversion of [(C₅Me₅)₂Ln][(μ-Ph)₂BPh₂] and KC₅Me₅ to (C₅Me₅)₃Ln, eq 6, is unsuccessful, it appears that pathways to these oxides from [(C₅Me₅)₂Ln][(μ-Ph)₂BPh₂] are facilitated during this synthetic step when there is more room around the metal.

The discovery of a fifth synthesis of (C₅Me₅)₃Sm, eq 8, indicates that synthetic approaches to these long-bond organometallic complexes are still evolving. Several of the successful syntheses used to make (C₅Me₅)₃Sm may seem obvious retrospectively, e.g., eq 6, but the example in eq 8 shows that we are still discovering these “obvious” routes.

Structure. Comparative structural data on **1–5** are of interest to determine if the metrical parameters would correlate with reactivity. Ultimately, it would be desirable to control reactivity by adjusting the metal size. Complexes **1–5** are isomorphous, and their metal–carbon and metal–(C₅Me₅ ring centroid) distances follow the differences in their ionic radii. The (C₅Me₅ ring centroid)⋯(C₅Me₅ ring centroid) distances also scale smoothly with the differences in ionic radii. Evidently the minimum spacing between three (C₅Me₅)[−] rings, i.e., the closest packing possible, has not yet been achieved in the **1–5** series. The out-of-plane displacements of the methyl carbons also increase regularly as the metal gets smaller and the rings pack more tightly, but the differences between complexes are small. These displacements range from 0.16 to 0.501 Å for the lanthanum complex, **1**, to 0.175–0.521 Å in the samarium complex, **5**, and show that there is considerable variation for the three crystallographically independent methyl carbon atoms in each structure.

Reactivity Comparisons as a Function of Metal Size. The data reported here suggest that (C₅Me₅)₃Ln reactivity correlates with steric crowding. (C₅Me₅)₃Sm, **5**, the sterically most crowded compound with the

smallest metal, is the most reactive with all substrates examined. (C₅Me₅)₃La, **1**, the least crowded compound with the largest metal, is the least reactive. These trends in reactivity apply to both η¹-alkyl reactivity, eq 2, and sterically induced reduction, eq 3.

For each type of (C₅Me₅)₃Ln reaction, the degree of differentiation of reactivity between the metals depends on the substrate. Hence, all of the (C₅Me₅)₃Ln complexes, **1–5**, react as η¹-alkyls with CO and THF, but the La reactions require more extreme conditions in terms of substrate concentration and reaction temperature. With ethylene and hydrogen as substrates, Sm and Nd are the most reactive, Ce and Pr require more forcing conditions, and La does not react at a detectable rate.

With the reducible substrates, Ph₃P=Se and C₈H₈, the chemistry of (C₅Me₅)₃Sm is distinct from that of the other four metals, which react similarly. Specifically, (C₅Me₅)₃Sm is able to reduce the selenium reagent to a selenide, (Se)^{2−}, whereas the less crowded complexes only form the perselenide, (Se₂)^{2−}. The reactivity of **1–4** is not further differentiated by this selenium reagent. (C₅Me₅)₃Sm reduces C₈H₈ to (C₈H₈)^{2−}, but the other (C₅Me₅)₃Ln complexes are unreactive with this substrate. AgBPh₄ and phenazine are reduced by all of the complexes in the series.

These reactions suggest that (C₅Me₅)₃Sm can reduce substrates with reduction potentials as negative as −1.83 V (C₈H₈) vs SCE, whereas (C₅Me₅)₃La has been demonstrated to reduce only at the −0.36 V vs SCE level. These numbers are at best approximate since the literature reduction potentials for the substrates will not match exactly the reduction of these species under these specific conditions. Moreover, if coordination of the substrate (or monoreduced substrate) to the metal occurs, the reduction potential will be further modified. This is particularly evident in the reductions of Ph₃P=Se, which has reported reduction potentials in the −2.145 to −2.690 V (vs SCE) range.^{93,94} Ideally, electrochemical studies on the (C₅Me₅)₃Ln complexes would give more definitive data. However, the high reactivity of these species makes this approach challenging. For example, THF and other polar solvents cannot be used, glassware must be silylated, and reactivity with supporting electrolytes is a concern.

New Reactivity Patterns. CO₂. The reaction of (C₅Me₅)₃Sm with CO₂, eq 21, demonstrates another special reaction of the (C₅Me₅)₃M complexes. CO₂ does not normally insert into (C₅Me₅)–M bonds, although it is commonly used to identify alkyl groups coordinated to electropositive metals. The fact that the CO₂ reaction occurs via formal insertion into an η¹-(C₅Me₅) group, eq 2, rather than by reduction to an oxalate, eqs 3 and 20, is likely related to the largely negative reduction potential, −2.21 V vs SCE, reported to be necessary for CO₂ reduction.⁸⁷ (C₅Me₅)₂Sm, which is established as a stronger reductant than **5**,⁸⁷ reduces CO₂, but with **5**, insertion is more facile.

Alkyl Halide Reactivity. Although (C₅Me₅)₃Sm reacts rapidly with alkyl halides, eq 23, the complexity

(93) Brennan, J. G.; Andersen, R. A.; Zalkin, A. *Inorg. Chem.* **1986**, *25*, 1761.

(94) Matschiner, V. H.; Tzschach, A.; Steinert, A. *Z. Anorg. Allg. Chem.* **1970**, *373*, 237.

of these reactions and the formation of multiple reaction products limit the amount of mechanistic information available. The presence of $(C_5Me_5)_2$ is consistent with sterically induced reduction chemistry, eq 3, and ring-opened products obtained from bromomethylcyclopropane indicate radical reactivity. However, the isolation of products such as C_5Me_5R shows that competing reactions involving nucleophilic displacement could also be operative. Since $(C_5Me_5)_3Sm$ is known to display both pseudo-alkyl reactivity and sterically induced reduction, the complexity of the product mixtures is not unreasonable. This is not surprising for another reason. Finke and co-workers have found the superficially simpler divalent $(C_5Me_5)_2Sm/RX$ systems ($X = \text{halide}$) are highly complicated as well. These reactions, using the known one-electron reductant, $(C_5Me_5)_2Sm$, form $[(C_5Me_5)_2SmX]_n$, $[(C_5Me_5)_3Sm_2X_3]_n$, and all the products expected from R radical reactions including C_5Me_5R .^{54,55}

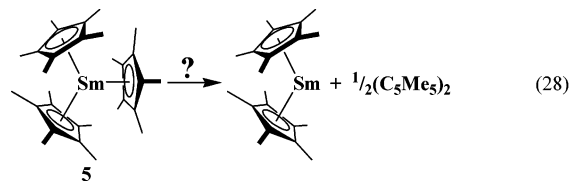
Aryl Halide Reactivity. The aryl halide reactions involving **1–5** are also complicated, but they provide information on several aspects of the reactivity of the $(C_5Me_5)_3Ln$ complexes. Comparisons of the $(C_5Me_5)_3Sm$ reactions with C_6H_5I and terphenyliodide suggest that both inner and outer sphere reductive reactivity are available. Since the C_6H_5I reaction is much faster, prior coordination seems likely in this case. Since the terphenyl reaction can occur, outer sphere pathways are possible.

The relative reactivity of $(C_5Me_5)_3Sm$ with C_6H_5X reagents follows the $X = I > Br > Cl > F$ order as expected. Although C_6H_5F is the least reactive, it does react. This attests to the high activity accessible via these long-bond organometallics. C–F activation is a challenging problem that has been approached from many directions.⁹⁵ Relatively few C–F activation reactions are known with lanthanides.^{90,96–101}

The aryl halide reactions also show how the reductive capacity of $(C_5Me_5)_3Ln$ complexes can be varied by changing the size of the metal. Although $(C_5Me_5)_3Sm$ readily reacts with chloro-, bromo-, and iodobenzene at room temperature, the less crowded $(C_5Me_5)_3Nd$ reacts only with C_6H_5I under these conditions and is so inert to C_6H_5Cl that it can be used as a solvent. The even less crowded $(C_5Me_5)_3Pr$ requires heating to react with C_6H_5I . Hence, with these substrates the reductive reactivity of the $(C_5Me_5)_3Ln$ complexes can be rather precisely adjusted by varying the metal size.

Activating Pentamethylcyclopentadienyl Reactivity via Steric Crowding. The reactivity demonstrated here shows clearly that the chemistry originally identified for $(C_5Me_5)_3Sm$ is not limited only to Sm and is not connected with the divalent oxidation state of this metal. Initially, it seemed possible that the reductive chemistry of $(C_5Me_5)_3Sm$ arose from homolytic

cleavage of one C_5Me_5 ring to form the $(C_5Me_5)_2Sm$ reductant, eq 28. Several lines of evidence argue against

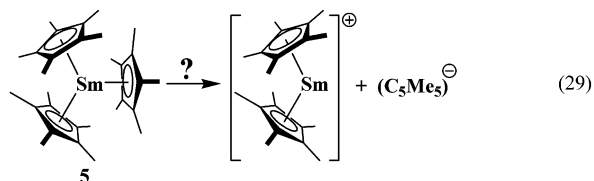


this. One example involves the difference in reactivity of $(C_5Me_5)_3Sm$ vs $(C_5Me_5)_2Sm$ with $PhN=NPh$. $(C_5Me_5)_3Sm$ reduces $PhN=NPh$ to the monoanion complex, $(C_5Me_5)_2Sm(PhNNPh)$,⁸ whereas the more powerful reductant $(C_5Me_5)_2Sm$ can reduce $PhN=NPh$ further to $[(C_5Me_5)_2Sm]_2(PhNNPh)$.^{102,103} The reaction of $(C_5Me_5)_3Sm$ with CO_2 also differs from that of $(C_5Me_5)_2Sm$. $(C_5Me_5)_2Sm$ reduces CO_2 to the oxalate $[(C_5Me_5)_2Sm]_2(\mu-O_2CCO_2)$, whereas $(C_5Me_5)_3Sm$ reacts to form the insertion product, $(C_5Me_5)_2Sm(O_2CC_5Me_5)$. If eq 28 were operative, these differences would not occur.

In addition, KC_5Me_5 reacts with $[(C_5Me_5)_2Sm][(\mu-Ph)_2BPh_2]$ to make $(C_5Me_5)_3Sm$, eq 7, rather than reducing Sm(III) to make $(C_5Me_5)_2Sm$, $KBPh_4$, and $(C_5Me_5)_2$. This indicates that $(C_5Me_5)^-$ is not a strong enough reductant to reduce Sm(III) to Sm(II), as would occur if $(C_5Me_5)_3Sm$ was converted to $(C_5Me_5)_2Sm$ and $(C_5Me_5)_2$, eq 28. Finally, this study showed that the reverse of eq 28, namely the reaction of $(C_5Me_5)_2Sm$ with $(C_5Me_5)_2$ to form $(C_5Me_5)_3Sm$, eq 8, is the favored direction of this reaction.

The demonstrated reactivity of **1–4** reinforces the assessment that homolytic cleavage is not the basis of the observed reactivity. If these complexes reacted via $(C_5Me_5)_2Ln$ intermediates, the La, Ce, and Pr complexes would be expected to be much more reactive than the Nd complex, which would still be more reactive than the Sm complex. This is based on the estimated Ln(III)/Ln(II) reduction potentials: La, -3.1 ; Ce, -3.2 ; Pr, -2.7 ; Nd, -2.6 ; Sm, -1.55 (V vs NHE).¹⁰⁴ This trend in reactivity is not observed.

The correlation of reactivity with steric crowding is consistent with the view that the $(C_5Me_5)^-$ ligands in these complexes are activated by placing them in a coordination environment in which they cannot obtain “normal” bonding distances. Located further from the metal, they cannot obtain their usual electrostatic stabilization and hence are more reactive. The chemical behavior of **1–5** also suggests that this reactivity is not just due to a $(C_5Me_5)^-$ ligand split heterolytically from $(C_5Me_5)_3Ln$, eq 29, to form a $[(C_5Me_5)_2Ln]^+$ cation and



$(C_5Me_5)^-$. Equation 29 could generate the observed

(95) Edelbach, B. L.; Fazlur Rahman, A. K.; Lachicotte, R. J.; Jones, W. D. *Organometallics* **1999**, *18*, 3170, and references therein.

(96) Deacon, G. B.; MacKinnon, P. I. *Tetrahedron Lett.* **1984**, *25*, 783.

(97) Deacon, G. B.; MacKinnon, P. I.; Tuong, T. D. *Aust. J. Chem.* **1983**, *36*, 43.

(98) Burns, C. J.; Andersen, R. A. *J. Chem. Soc., Chem. Commun.* **1989**, 136.

(99) Evans, W. J.; Giarikos, D. G.; Johnston, M. A.; Greci, M. A.; Ziller, J. W. *J. Chem. Soc., Dalton Trans.* **2002**, 520.

(100) Deacon, G. B.; Forsyth, C. M. *Organometallics* **2003**, *22*, 1349.

(101) Maron, L.; Werkema, E. L.; Perrin, L.; Eisenstein, O.; Andersen, R. A. *J. Am. Chem. Soc.* **2005**, *127*, 279.

(102) Evans, W. J.; Drummond, D. K.; Bott, S. G.; Atwood, J. L. *Organometallics* **1986**, *5*, 2389.

(103) Evans, W. J.; Drummond, D. K.; Chamberlain, L. R.; Doedens, R. J.; Bott, S. G.; Zhang, H.; Atwood, J. L. *J. Am. Chem. Soc.* **1988**, *110*, 4983.

(104) Morss, L. R. *Chem. Rev.* **1976**, *76*, 827.

reduction products, since the (C₅Me₅)⁻ ion could reduce the substrate, leaving half an equivalent of (C₅Me₅)₂. However, if this were the case, **1–5** should have identical reductive reactivity, namely, that of the isolated (C₅Me₅)⁻ anion. Since complexes **1–5** display different reactivity, eq 29 cannot explain the results.

Collectively these data indicate that a normally inert, ancillary ligand can be activated to have a broad range of reactivity by placing it in a coordination environment in which it cannot achieve its normal metal ligand bonding distance. Moreover, the reactivity can be tuned by varying the degree of steric crowding. It should be noted that only small differences in steric factors can cause the crossover of a normally inert ligand to a reactive species. Hence, removal of one methyl group per cyclopentadienyl ring appears to eliminate this high reactivity: (C₅Me₄H)₃M complexes have not displayed the reactivity observed for (C₅Me₅)₃M.^{13,14} A more striking example is the ansa complex [Me₂Si(C₅Me₄)₂]Sm-(C₅Me₅). The silyl bridge pulls the two rings in the ansa ligand further apart, making the complex less crowded. The compound has normal Sm–C(C₅Me₅) distances and none of the special reactivity of (C₅Me₅)₃Sm.²¹

A referee has correctly pointed out that the tendency of these (C₅Me₅)₃Ln complexes to display η¹-C₅Me₅ reactivity makes them appear to behave more like main group cyclopentadienyl complexes, for which η¹ structures and reactivity has been known for years.¹⁰⁵ For example, isocyanides have been shown to insert into Al–C(C₅Me₄H) bonds¹⁰⁶ and Be–(C₅Me₅) linkages.¹⁰⁷ η¹-C₅Me₅ migration from phosphorus and silicon to other elements has also been observed.^{105,108,109} It should also be noted that under the proper conditions (C₅H₅)⁻ ligands attached to transition metals can display η¹ reactivity as demonstrated by the conversion of (C₅H₅)-Re(CO)(NO)Me to the cyclopentadienylideneketene (C₅H₄CO)Re(NO)(PMe₃)₃ upon addition of excess PMe₃ and loss of H from (C₅H₅)⁻ as CH₄.^{110,111} This η⁵ to η¹ conversion may have an origin similar to the reactivity of the (C₅Me₅)₃Ln complexes in that it may occur due to an increase in steric congestion caused by addition of the PMe₃ ligands.

Reductive Chemistry for Trivalent Lanthanide Complexes. The reductive chemistry demonstrated for the trivalent (C₅Me₅)₃Ln complexes, **1–5**, demonstrates that steric crowding can transform complexes of redox inactive metals into reducing agents. The influence of these steric factors on redox reactivity is unusual since redox chemistry is normally controlled by varying the electronic aspects of the ligands in a metal complex, not

the steric features. This sterically induced reduction reactivity brings much of the reductive chemistry, which has proven to be so powerful for Sm, to all of the larger metals. This will be useful in several ways as described in the following paragraphs.

Extending Sm(II) reductive chemistry to the larger lanthanides will allow size optimization of lanthanide reductive chemistry. Although there are many successful Sm(II) reductions in the literature, there are also many substrates that react with (C₅Me₅)₂Sm but did not give fully characterizable products since the NMR spectra of these paramagnetic species were not definitive and crystals were not obtained. These reductions can now be examined with the larger metals to see if more crystalline products will result and with La to allow full utilization of NMR spectroscopy.

Sterically induced reduction will also lead to a broader development of the chemistry of La–Nd. Complexes previously obtainable only from Sm(II) can now be made with these other metals. This is particularly advantageous with diamagnetic La(III) and with Nd(III), which is often the favored metal for catalytic isoprene polymerization.¹¹²

The fact that this reductive reactivity can be varied by the degree of steric crowding provides an additional benefit. Previously, with the divalent (C₅Me₅)₂Sm and (C₅Me₅)₂Sm(THF)₂ systems, there was little opportunity to vary the reduction potential to direct which trivalent Sm products formed. With the (C₅Me₅)₃Ln complexes, and with further variation of the metal/ligand size ratio, more precise control of the reducing capacity should be possible.

Conclusion

The sterically crowded (C₅Me₅)₃Ln complexes are now synthetically accessible for all of the large lanthanides, La–Nd, as well as for (C₅Me₅)₃Sm. The reactivity of this series of long bond organometallic species shows that the normally inert (C₅Me₅)⁻ ligand can be transformed into a reactive ligand via steric crowding. Reactivity increases with increased steric crowding in both η¹-alkyl and sterically induced reduction reactions, the two main patterns identified so far for (C₅Me₅)₃Ln complexes. The differences in reactivity as a function of metal size depend on the specific substrate and reaction. This reactivity allows size optimization of lanthanide reductive chemistry and an expansion to La–Nd of the chemistry previously accessible only to Sm(II).

Acknowledgment. We are grateful to the National Science Foundation for support of this project.

Supporting Information Available: X-ray diffraction data, atomic coordinates, thermal parameters, and complete bond distances and angles for **2**, **3**, and **6–10**; listing of observed and calculated structure factor amplitudes (PDF). This material is available free of charge via the Internet at <http://pubs.acs.org>.

OM050402L

(112) Evans, W. J.; Giarikos, D. G.; Allen, N. T. *Macromolecules* **2003**, *36*, 4256, and references therein.

(105) Jutzi, P.; Reumann, G. *J. Chem. Soc., Dalton Trans.* **2000**, 2237.

(106) Shapiro, P. J.; Vij, A.; Yap, G. P. A.; Rheingold, A. L. *Polyhedron* **1995**, *14*, 203.

(107) Carmona, E.; del Mar Conejo, M.; Fernández, R.; Andersen, R. A.; Gutiérrez-Puebla, E.; Monge, M. A. *Chem. Eur. J.* **2003**, *9*, 4462.

(108) Jutzi, P.; Meyer, U.; Opiela, S.; Neumann, B.; Stammler, H. G. *J. Organomet. Chem.* **1992**, *439*, 279.

(109) Holtmann, U.; Jutzi, P.; Kühler, T.; Neumann, B.; Stammler, H. G. *Organometallics* **1999**, *18*, 5531.

(110) Casey, C. P.; O'Connor, J. M. *J. Am. Chem. Soc.* **1983**, *105*, 2919.

(111) Casey, C. P.; O'Connor, J. M.; Haller, K. J. *J. Am. Chem. Soc.* **1985**, *107*, 1241.